

Structure–Activity Relationship of a New Series of Reversible Dual Monoacylglycerol Lipase/Fatty Acid Amide Hydrolase Inhibitors

José A. Cisneros,[†] Emmelie Björklund,[‡] Inés González-Gil,[†] Yanling Hu,[‡] Ángeles Canales,[†] Francisco J. Medrano,[§] Antonio Romero,[§] Silvia Ortega-Gutiérrez,[†] Christopher J. Fowler,[‡] and María L. López-Rodríguez^{*,†}

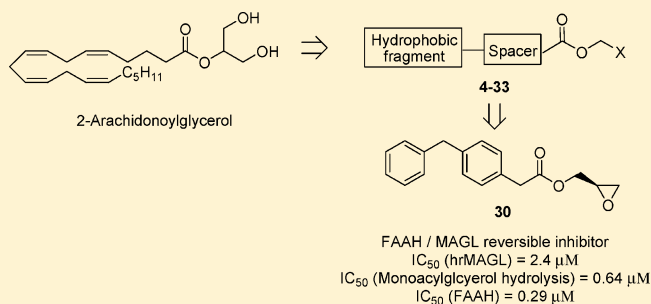
[†]Departamento de Química Orgánica I, Facultad de Ciencias Químicas, Universidad Complutense de Madrid, E-28040 Madrid, Spain

[‡]Department of Pharmacology and Clinical Neuroscience, Umeå University, Umeå, Sweden

[§]Departamento de Biología Físico-Química, Centro de Investigaciones Biológicas, Consejo Superior de Investigaciones Científicas, E-28040 Madrid, Spain

S Supporting Information

ABSTRACT: The two endocannabinoids, anandamide (AEA) and 2-arachidonoylglycerol (2-AG), play independent and nonredundant roles in the body. This makes the development of both selective and dual inhibitors of their inactivation an important priority. In this work we report a new series of inhibitors of monoacylglycerol lipase (MAGL) and fatty acid amide hydrolase (FAAH). Among them, (\pm)-oxiran-2-ylmethyl 6-(1,1'-biphenyl-4-yl)hexanoate (**8**) and (2*R*)-(-)-oxiran-2-ylmethyl(4-benzylphenyl)acetate (**30**) stand out as potent inhibitors of human recombinant MAGL (IC_{50} (**8**) = 4.1 μ M; IC_{50} (**30**) = 2.4 μ M), rat brain monoacylglycerol hydrolysis (IC_{50} (**8**) = 1.8 μ M; IC_{50} (**30**) = 0.68 μ M), and rat brain FAAH (IC_{50} (**8**) = 5.1 μ M; IC_{50} (**30**) = 0.29 μ M). Importantly, and in contrast to the other previously described MAGL inhibitors, these compounds behave as reversible inhibitors either of competitive (**8**) or noncompetitive nature (**30**). Hence, they could be useful to explore the therapeutic potential of reversible MAGL inhibitors.



INTRODUCTION

Endocannabinoids (eCBs) constitute a class of lipid messengers that exert their biological actions through the interaction with two G protein-coupled cannabinoid receptors, CB₁ and CB₂. These components, together with the enzymes responsible for the biosynthesis and degradation of eCBs, constitute the endogenous cannabinoid system which regulates a broad spectrum of physiological processes, such as pain, inflammation, feeding behavior, and neurodegeneration.^{1,2} The main eCBs are *N*-arachidonylethanolamine (anandamide, AEA) and 2-arachidonoylglycerol (2-AG), and these ligands play separate and tightly regulated roles in the body, rather than simply acting as alternate ligands for the same receptors.³

AEA and 2-AG are primarily metabolized by hydrolysis to arachidonic acid. While the role of FAAH as the key enzyme in AEA inactivation is well established,⁴ several enzymes are responsible for 2-AG inactivation, of which monoacylglycerol lipase (MAGL) is the key hydrolytic enzyme. About 85% of the total 2-AG hydrolysis in the brain has been ascribed to MAGL, while the remaining activity is mainly due to the activities of α/β hydrolase-6 (ABHD-6) and α/β hydrolase-12 (ABHD-12).⁵

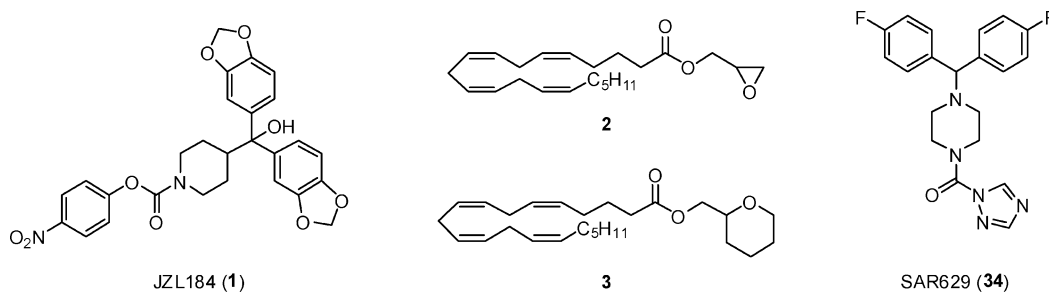
The central roles of FAAH and MAGL in gating eCB levels make them promising targets for drug development. A wide variety of FAAH inhibitors have been described, not least by

the pharmaceutical industry.⁶ MAGL inhibitor pharmacology lagged behind until the discovery of JZL184 (**1**, Chart 1).⁷ This compound, which acts as an irreversible inhibitor, has been used to explore the therapeutic potential of MAGL, primarily in pain states.^{7,8} However, chronic enhancement of 2-AG levels produced either by repeated treatment with **1** or by genetic deletion of MAGL induces desensitization of the CB₁ receptors and impairs 2-AG-mediated antinociceptive effects.⁹ At first sight, this finding argues against the therapeutic exploitation of MAGL inhibition. However, both genetic deletion of MAGL and the use of an irreversible inhibitor of the enzyme represent a sustained loss of MAGL activity, raising the possibility that reversible MAGL inhibitors will not produce such desensitization. No potent MAGL reversible inhibitors, however, have, to our knowledge, been characterized. In the present study, we report the design and synthesis of a new series of biphenyl, 4-phenylbenzyl, and 4-phenylethylphenyl derivatives and their ability to inhibit human recombinant MAGL (hrMAGL) as well as their capacity to interfere with 2-oleoylglycerol (2-OG, an alternate MAGL substrate) and AEA hydrolysis in brain homogenates. Among the synthesized compounds, derivatives

Received: October 4, 2011

Published: December 21, 2011

Chart 1. Structure of the Monoacylglycerol Lipase (MAGL) Inhibitors JZL184 (1), UCM162 (2), UCM505 (3), and SAR629 (34)



8 and 30 show good potency toward MAGL and do not produce the sort of time-dependent inhibition seen with irreversible inhibitors. These compounds could open new perspectives for modulating MAGL activity and to assess whether reversible inhibition is a strategy with which to exploit the therapeutic potential of this enzyme.

RESULTS AND DISCUSSION

Design. In a previous study¹⁰ we identified oxiran-2-ylmethyl (5*Z*,8*Z*,11*Z*,14*Z*)-icosa-5,8,11,14-tetraenoate (2) and tetrahydro-2*H*-pyran-2-ylmethyl (5*Z*,8*Z*,11*Z*,14*Z*)-icosa-5,8,11,14-tetraenoate (3) as inhibitors of monoacylglycerol hydrolysis (Chart 1). However, these compounds were based on the structure of 2-AG, and thereby, they retain the arachidonic acid chain in their structure. This moiety could be prone to oxidation in biological media, and it may limit the selectivity of the compounds, given that arachidonic acid is a key metabolite in several pathways and therefore can be recognized by different enzymes, including an assortment of lipases and cyclooxygenases. Hence, we sought to replace the arachidonic acid moiety with a suitable bioisostere. Optimally, the selected group should be stable in biological settings and chemically versatile to enable structure exploration. Since the biphenyl group has been suggested as an isostere of arachidonic acid,¹¹ we envisioned a series of esters that contained a biphenyl core and the heterocyclic moieties previously optimized. Since our data indicate that derivative 2 behaves as a competitive inhibitor (unpublished observations), it is conceivable that its carbonyl group is placed close to the catalytic serine (Ser 132) of the enzyme. On the basis of the recently reported 3D structure of MAGL,^{12,13} an important site of interaction in addition to the active site is the hydrophobic pocket defined by the side chains of residues Leu 158, Ala 174, Leu 186, Ile 189, Leu 215, Val 217, Ile 221, Leu 223, and Leu 224. Therefore, we carried out docking studies in order to obtain some clues about whether the introduction of a suitable spacer between the biphenyl core and the oxygenated ring or between both benzene rings of the biphenyl group could facilitate the simultaneous interaction of the compound with the catalytic serine and the hydrophobic pocket.

Docking calculations have been performed by using Glide software^{14,15} as described in the Experimental Section. Docking results suggest that the incorporation of a spacer with five methylenic units between the carbonyl group and the biphenyl system (Figure 1A) or of one methylene between the two benzene rings and a spacer of three methylenes between the carbonyl group and the first phenyl ring (Figure 1B) allows for the favorable hydrophobic interactions of the aromatic rings of the compounds and the hydrophobic pocket while keeping the

carbonyl group at the adequate distance and orientation to interact with the catalytic serine.

Glide docking of the derivative with five methylenic units between the carbonyl group and the biphenyl system (compound 8) into the active site of MAGL afforded three binding poses. In all of them, the catalytic serine (Ser 132) is located in the vicinity of the carbonyl of 8 and the methylenic chain attached to the biphenyl group points toward the exit of the channel where the hydrophobic residues that interact with the arachidonoyl moiety of 2-AG are located. The refined model of the less energy binding pose obtained with Prime¹⁶ (Figure 1A) shows a hydrogen bond between the oxygen atom of the ester carbonyl and the backbone NH of Ala 61. A similar hydrogen bond was found between the carbonyl oxygen of the MAGL covalent inhibitor SAR629 (34, Chart 1) and Ala 61 in the crystal structure of the complex, and it was also proposed in the docking models described for the natural substrates (2-AG and 1(3)-AG).¹³ In our case, the biphenyl group interacts mainly with the hydrophobic residues Leu 158, Ala 174, Leu 186, Leu 215, Ile 221, Leu 223, and Leu 224, which are also involved in van der Waals contacts with the fluorophenyl rings of inhibitor 34 in the crystal structure.¹³ Therefore, according to docking calculations, compound 8 could be recognized by MAGL occupying the channel where the natural substrate should be accommodated.

Docking calculations carried out with the derivative with one methylene between the two benzene rings and a spacer of three methylenes between the carbonyl group and the first phenyl ring (compound 22) yielded a similar binding mode to the docking pose obtained for 8, with the carbonyl group of 22 located near the nucleophilic oxygen atom of the catalytic serine (Figure 1B). The main difference with 8 is the location of the oxirane ring of the molecule, which is more buried into the polar pocket of the enzyme in the case of compound 22 than in compound 8. Due to this disposition and the shorter length of the spacer, it is possible that this compound would establish fewer interactions with the hydrophobic residues of the enzyme channel than derivative 8, since residues Ala 174, Leu 186, Ile 221, and Leu 215 are not directly involved in ligand recognition.

According to these computational models, we designed two different series of derivatives 4–33 (Figure 1C) where the lipophilic moiety has been substituted by biphenyl, 4-benzylphenyl (Y = CH₂), and 4-phenylethylphenyl (Y = CH₂CH₂) groups.

Chemistry, Biological Evaluation, and Structure–Activity Relationship (SAR) Study. The synthesis of the esters 4–31 is indicated in Scheme 1. In general, appropriate commercially available or previously synthesized carboxylic

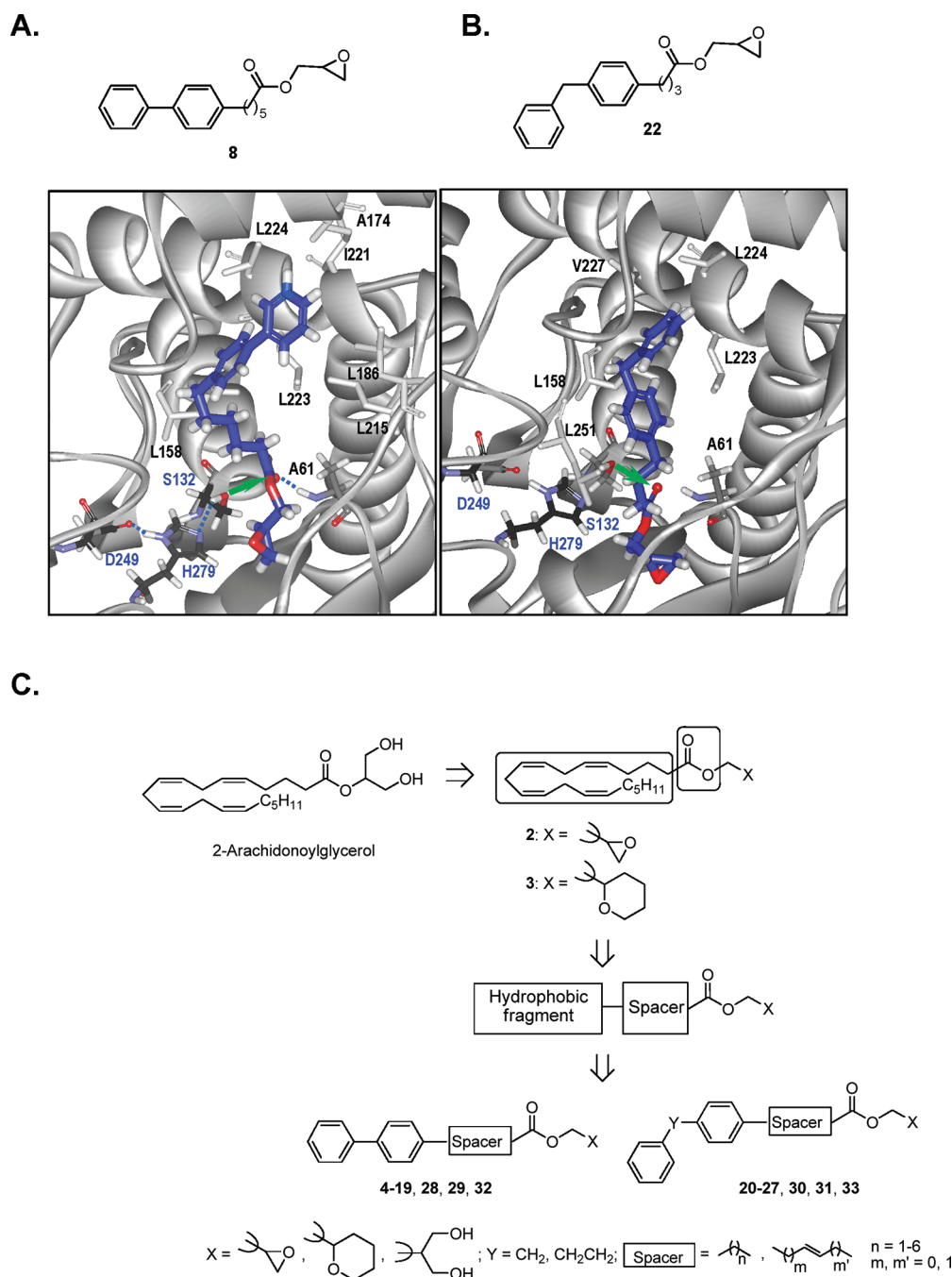
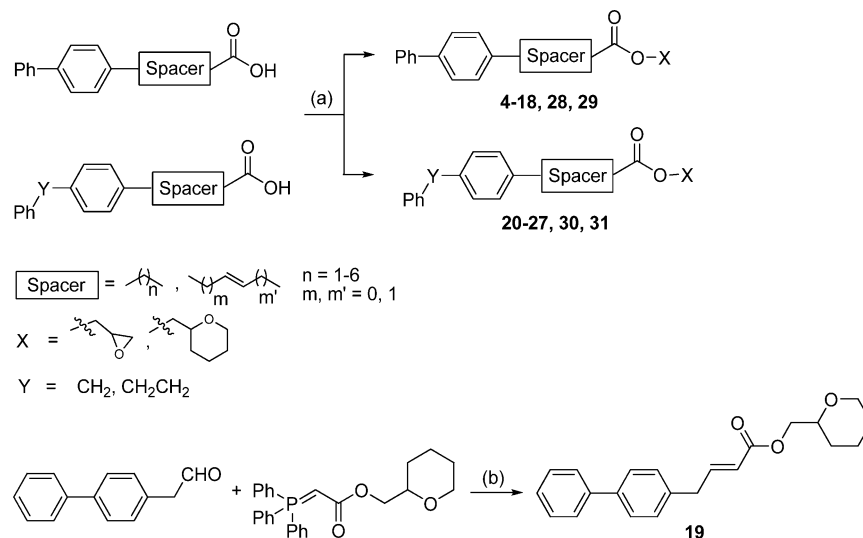


Figure 1. Computational models of the complexes between compounds (A) **8** and (B) **22** and MAGL (PDB code 3JW8). Residues of the catalytic triad have been labeled in blue. The hydroxyl group of Ser 132 and the carbonyl group of the compounds are marked with an arrow (in green). Shown models correspond to the *R* enantiomer for compound **8** and to the *S* enantiomer for compound **22**. (C) Design of compounds **4–33**.

acids were condensed with the corresponding alcohol in the presence of dicyclohexylcarbodiimide (DCC) and catalytic amounts of *N,N*-dimethyl-4-aminopyridine (DMAP), except compound **19**, which has been prepared by Wittig reaction between tetrahydro-2*H*-pyran-2-ylmethyl (triphenylphosphoranylidene)acetate and (1,1'-biphenyl-4-yl)-acetaldehyde.

Final compounds **4–31** were tested not only for their ability to inhibit MAGL activity *in vitro* but also for their capacity to block 2-OG hydrolysis in brain homogenates, since the most interesting compounds are those that can inhibit both hrMAGL *in vitro* and also monoacylglycerol hydrolysis in rat brain, since

this would allow the compound to be used in biologically more relevant studies. Furthermore, in view of our previous finding that some compounds (such as troglitazone) show assay dependency in their ability to inhibit MAGL,¹⁷ it is important to demonstrate that active compounds are active regardless of the MAGL assay used. The hrMAGL inhibition assay was carried out as previously reported¹⁸ with some modifications¹⁷ using commercially available his-tagged hrMAGL. The capacity of the compounds to interfere with the hydrolysis of 2-AG in cytosolic fractions was determined using 2-oleoylglycerol (2-OG) as a surrogate. Effects upon the FAAH-catalyzed hydrolysis of AEA by the membrane fractions were also

Scheme 1. Synthesis of Derivatives 4–31^a

^aReagents and conditions: (a) X-OH, DCC, DMAP, CH_2Cl_2 , Ar, rt; (b) toluene, Δ .

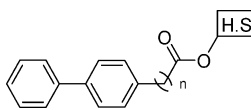
determined to characterize the selectivity of the compounds for MAGL vs FAAH. 2-OG and AEA hydrolytic activities were measured using a substrate concentration of $0.5 \mu\text{M}$ and the assay procedures described previously using membrane and cytosolic fractions of rat cerebella.¹⁹ These results are shown in Tables 1–4. For consistency of notation, throughout the tables, IC_{50} and pI_{50} values for hrMAGL, 2-OG, or AEA hydrolysis inhibition are denoted as hrMAGL, 2-OG, and AEA, respectively. In some cases, 100% inhibition was not seen at the highest dose tested. This type of situation is indicated throughout the tables by adding the percentage of maximum inhibition value obtained for the highest concentration tested ($10 \mu\text{M}$ for hrMAGL or $100 \mu\text{M}$ for 2-OG or AEA hydrolysis).

Influence of the Spacer. First, we analyzed the effect of the length of the spacer in the biphenyl derivatives 4–15 (Table 1) on the endocannabinoid hydrolysis inhibition. In general, for oxirane esters 4–9, increasing the length of the methylenic spacer enhances the inhibitory activity of the compounds at hrMAGL, from no or low inhibition (for compounds 4 and 5) to IC_{50} values between 1.8 and $6.6 \mu\text{M}$ (compounds 6–8, with spacers of 3 to 5 methylenic units, respectively). Further elongation decreases inhibition of hrMAGL, as shown by derivative 9 (11% inhibition at $10 \mu\text{M}$). Given the importance of the fact that compounds which behave as *in vitro* hrMAGL inhibitors also show the capacity to block monoacylglycerol hydrolysis in the brain, the results obtained in brain cytosolic fractions using 2-OG as a 2-AG surrogate highlight the importance of compounds 7 [IC_{50} (hrMAGL) = $6.6 \mu\text{M}$; IC_{50} (2-OG) = $2.6 \mu\text{M}$] and 8 [IC_{50} (hrMAGL) = $4.1 \mu\text{M}$; IC_{50} (2-OG) = $1.8 \mu\text{M}$]. The effect of the length of the spacer of oxirane derivatives 4–9 on FAAH inhibition shows, however, an opposite trend, with the shortest spacers ($n = 1-3$, compounds 4–6) being the ones that yielded the lowest IC_{50} values (0.59 , 0.87 , and $0.71 \mu\text{M}$, respectively). When the heterocyclic subunit is a tetrahydropyran ring (derivatives 10–15), no significant simultaneous inhibition for hrMAGL and for 2-OG hydrolysis inhibition was observed for any of them [IC_{50} (2-OG) > $100 \mu\text{M}$]. These compounds showed, nonetheless, a moderate potency as FAAH inhibitors, with IC_{50} values ranging from $3.9 \mu\text{M}$ (compound 15) to 20

μM (compound 13). Next, we studied whether the presence of one unsaturation of *trans* geometry in the spacer could be favorable for the inhibition of MAGL activity and AEA hydrolysis (Table 2). None of the synthesized compounds (16–19), regardless of the presence of oxirane or tetrahydropyran as heterocyclic subunit, showed any significant capacity to block concomitantly hrMAGL activity and 2-OG hydrolysis. It is interesting to note, however, the good capacity of derivatives 16 and 17 to inhibit hrMAGL (IC_{50} values of 5.1 and $0.76 \mu\text{M}$, respectively). With respect to FAAH, only 16 showed a moderate activity toward FAAH inhibition with an IC_{50} value of $3.8 \mu\text{M}$. In sum, among all these biphenyl derivatives 4–19, compounds 7 and 8 are the most potent inhibitors of the series. Furthermore, derivative 8, which is more potent than initial hits 2 and 3 to inhibit 2-OG hydrolysis [IC_{50} (8) = $1.8 \mu\text{M}$; IC_{50} (2) = $4.5 \mu\text{M}$; IC_{50} (3) = $5.6 \mu\text{M}$], acts directly at MAGL [IC_{50} (8, hrMAGL) = $4.1 \mu\text{M}$], and lacks the arachidonic acid chain in its structure.

Modifications in the Biphenyl Moiety. Taking into account the docking models (Figure 1B) and the previous results, we also studied the possibility of replacing the biphenyl moiety for two benzene rings separated by different spacers (one or two methylenic units) and decreasing the length chain that separates the hydrophobic moiety and the heterocyclic subunit (Table 3) in compounds 20–27. Only the oxirane derivative 20, with one methylenic unit between the two benzene rings and one methylenic unit in the spacer ($m, n = 1$), showed a significant capacity to inhibit hrMAGL (IC_{50} value of $16 \mu\text{M}$) and 2-OG hydrolysis (IC_{50} value of $10 \mu\text{M}$). Nonetheless, some of the oxirane esters with one methylenic unit between the two benzene rings ($m = 1$) exhibited some capacity to block 2-OG hydrolysis [IC_{50} (21) = $19 \mu\text{M}$; IC_{50} (22) = $8 \mu\text{M}$], a result that suggests that these compounds may be able to distinguish between MAGL activities in different species or between distinct 2-OG hydrolyzing activities. The increase of the length of the linker between the two benzene rings to two methylenic units ($m = 2$) abolished all activity, as shown by compound 23, where only 18% inhibition at the maximal concentration tested was observed for 2-OG hydrolysis and resulted inactive at hrMAGL. Regarding the

Table 1. Influence of the Length of the Spacer



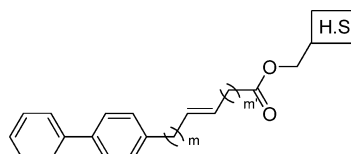
Cpd	H.S.	n	Hydrolysis inhibition pI ₅₀ [IC ₅₀ , μM] ^a		
			hrMAGL	2-OG	AEA
4		1	n.i. ^b	<4 (44±3%) ^c	6.23±0.02 [0.59]
5		2	<5 (22±5%) ^c	<4 (25±3%) ^c	6.06±0.02 [0.87]
6		3	5.73±0.08 [1.8, 86±6%] ^d	<4 (46±3%) ^c	6.15±0.02 [0.71]
7		4	5.18±0.05 [6.6]	5.58±0.05 [2.6, 87±3] ^d	5.33±0.03 [4.6]
8		5	5.39±0.06 [4.1]	5.73±0.03 [1.8, 89±2] ^d	5.29±0.03 [5.1]
9		6	<5 (11±5%) ^c	<4 (16±4%) ^c	5.50±0.03 [3.2]
10		1	<5 (21±5%) ^c	<4 (33±2%) ^c	4.80±0.05 [16]
11		2	5.81±0.07 [1.6, 67±5] ^d	<4 (50±2%) ^c	4.82±0.04 [15]
12		3	<5 (34±4%) ^c	n.i. ^b	4.93±0.01 [12]
13		4	4.92±0.07 [12]	<4 (13±7%) ^c	4.70±0.05 [20]
14		5	<5 (33±2%) ^c	<4 (27±2%) ^c	4.94±0.05 [12, 60±4%] ^d
15		6	<5 (37±2%) ^c	<4 (47±4%) ^c	5.41±0.07 [3.9, 83±4%] ^d

^aThroughout the tables, the pI₅₀ values (−log₁₀ [IC₅₀]) are expressed as mean ± s.e.m., and they are calculated from data obtained in 3–10 independent experiments. The IC₅₀ values derived from the mean pI₅₀ values are given in brackets. ^bn.i. indicates <10% inhibition at the highest concentration tested (10 μM for hrMAGL or 100 μM for 2-OG or AEA hydrolysis). ^cWhen the inhibitable component was less than 50%, when the data could not be fitted to a curve due to a marginal degree of inhibition, or when the pI₅₀ value was lower (and hence the IC₅₀ value higher) than the highest concentration tested (10 μM for hrMAGL or 100 μM for 2-OG or AEA hydrolysis), the pI₅₀ values have been indicated as <5 or <4 (i.e., IC₅₀ value >10 μM or IC₅₀ value >100 μM, respectively), and the percentage of inhibition attained at 10 or 100 μM has been indicated between parentheses as mean ± s.e.m. ^dWhen the data was better fitted to an inhibition curve with a residual activity (i.e., the “bottom” value) >0, the percentage of inhibitable component (100−“bottom” value) is given in the table as maximum inhibition and the data expressed as pI₅₀ [IC₅₀, percentage of maximum inhibition].

tetrahydropyran derivatives **24–27**, none of the modifications yielded significant inhibition values for either 2-OG hydrolysis or hrMAGL activity (Table 3). With respect to FAAH inhibition, in general, all these compounds were able to inhibit AEA hydrolysis, with moderate IC₅₀ values between 0.28 and 50 μM.

Influence of the Stereogenic Center. In summary, from all synthesized compounds **4–27**, the ones with the best inhibitory profile toward 2-AG hydrolysis were the biphenyl derivative **8** [IC₅₀ (hrMAGL) = 4.1 μM; IC₅₀ (2-OG) = 1.8 μM] and the 4-benzylphenyl derivative **20** [IC₅₀ (hrMAGL) = 16 μM; IC₅₀ (2-OG) = 10 μM]. Since both of them contain a stereogenic center, we next studied its influence by synthesizing the two enantiomers of **8** (derivatives **28** and **29**) and **20** (**30** and **31**). The results compiled in Table 4 indicated that the

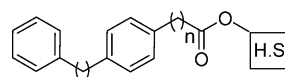
Table 2. Influence of Unsaturation in the Spacer



Cpd	m	m'	H.S.	Hydrolysis inhibition pI ₅₀ [IC ₅₀ , μM] ^a		
				hrMAGL	2-OG	AEA
16	0	0		5.29±0.07 [5.1]	n.i. ^b	5.42±0.03 [3.8, 73±2%] ^d
17	0	0		6.12±0.05 [0.76, 90±4%] ^d	n.i. ^b	<4 (37±1%) ^c
18	0	1		<5 (12±2%) ^c	<4 (34±7%) ^c	4.66±0.09 [22]
19	1	0		<5 (49±3%) ^c	<4 (19±9%) ^c	4.80±0.07 [16, 59±4%] ^d

^aFor an explanation of the data, see the footnotes for Table 1.

Table 3. Influence of the 4-Benzylphenyl and 4-Phenylethylphenyl Moieties



Cpd	m	n	H.S.	Hydrolysis inhibition pI ₅₀ [IC ₅₀ , μM] ^a		
				hrMAGL	2-OG	AEA
20	1	1		4.81±0.07 [16]	4.99±0.02 [10]	6.56±0.01 [0.28]
21	1	2		n.i. ^b	4.73±0.05 [19, 72±4%] ^d	5.64±0.03 [2.3]
22	1	3		<5 (29±5%) ^c	5.10±0.05 [8.0, 86±3%] ^d	5.44±0.03 [3.6]
23	2	0		n.i. ^b	<4 (18±2%) ^c	4.55±0.03 [28]
24	1	1		n.i. ^b	<4 (25±5%) ^c	5.17±0.02 [6.8, 96±2%] ^d
25	1	2		n.i. ^b	<4 (41±1%) ^c	5.01±0.02 [9.7]
26	1	3		<5 (14±6%) ^c	<4 (13±1%) ^c	4.93±0.04 [12, 72±3] ^d
27	2	0		n.i. ^b	n.i. ^b	4.30±0.04 [50]

^aFor an explanation of the data, see the footnotes for Table 1.

stereogenic center does not exert a great influence in the inhibitory ability of compounds **28** and **29**, with close IC₅₀ values for 2-OG hydrolysis of 1.8 μM (racemic **8**), 4.9 μM (*R*-enantiomer **28**), and 5.1 μM (*S*-enantiomer **29**). Both enantiomers inhibited hrMAGL, but <50% inhibition was seen at the highest concentration tested (10 μM), precluding determination of their IC₅₀ values. In contrast, the configuration of the stereogenic center plays an important role in the case of the 4-benzylphenyl derivative **20**, where a remarkable difference between the activities of both enantiomers can be observed. While *S*-enantiomer **31** showed a lack of activity at hrMAGL or a low inhibitory capacity in cytosolic brain fractions [IC₅₀(2-OG) = 70 μM] compared with the racemic **20** [IC₅₀(hrMAGL) = 16 μM; IC₅₀(2-OG) = 10 μM], its *R*-counterpart **30** behaves as a potent inhibitor of hrMAGL (IC₅₀ = 2.4 μM) and of 2-OG hydrolysis with an IC₅₀ value in the submicromolar range (0.68 μM). No such stereoselectivity was seen for the inhibition of AEA hydrolysis by FAAH.

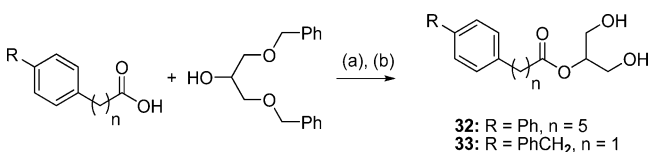
Table 4. Influence of the Stereogenic Center and the Glycerol Moiety in Derivatives 8 and 20

Cpd	X	Hydrolysis inhibition pI ₅₀ [IC ₅₀ , μM] ^a			Cpd	X	Hydrolysis inhibition pI ₅₀ [IC ₅₀ , μM] ^a		
		hrMAGL	2-OG	AEA			hrMAGL	2-OG	AEA
8		5.39±0.06	5.73±0.03	5.29±0.03	20		4.81±0.07	4.99±0.02	6.56±0.01
		[4.1]	[1.8, 89±2%] ^d	[5.1]			[16]	[10]	[0.28]
28		<5	5.31±0.03	5.41±0.01	30		5.61±0.02	6.17±0.03	6.54±0.01
		(33±5%) ^c	[4.9, 91±2%] ^d	[3.9]			[2.4]	[0.68]	[0.29]
29		<5	5.29±0.03	5.35±0.02	31		n.i. ^b	4.15±0.09	6.47±0.01
		(45±5%) ^c	[5.1, 92±2%] ^d	[4.5, >95] ^d				[70]	[0.34]
32		5.12±0.02	5.81±0.07	5.73±0.02	33		n.i. ^b	<4	6.15±0.02
		[7.5]	[1.5, 91±3] ^d	[1.9, >95] ^d				(49±2%) ^c	[0.70]

^aFor an explanation of the data, see the footnotes for Table 1.

Replacement of the Oxirane Group with the 2-Glycerol Moiety. Finally, and in an attempt to further optimize the potency of 8 and 20 to inhibit 2-OG hydrolysis, we have replaced their oxirane ring with the 2-glycerol moiety, present in the molecule of 2-AG. Derivatives 32 and 33 were obtained through esterification of the corresponding carboxylic acids with 1,3-dibenzyloxypropan-2-ol followed by deprotection of the hydroxyl groups by catalytic hydrogenation in the presence of palladium hydroxide (Scheme 2). The activity

Scheme 2. Synthesis of Derivatives 32 and 33^a



^aReagents and conditions: (a) DCC, DMAP, CH₂Cl₂, Ar, rt; (b) Pd(OH)₂, CH₂Cl₂/EtOH, rt.

assays (Table 4) showed that this modification did not significantly affect the inhibitory ability of 32 when compared with its analogue 8, with IC₅₀ values for hrMAGL inhibition of 7.5 and 4.1 μM, respectively, and 2-OG hydrolysis inhibition of 1.5 and 1.8 μM, respectively (Table 4). On the contrary, the same modification basically abolished the activity of the parent compound 20 in both assays. Derivative 33 did not inhibit hrMAGL whereas 20 had an IC₅₀ value of 16 μM and similarly, for 2-OG hydrolysis, 33 showed only a 49% inhibition at 100 μM, whereas 20 had an IC₅₀ value of 10 μM.

In summary, from the SAR study, compounds 8 and 30 exhibited the best inhibitory profiles (see Figure 2 for representative curves) and were therefore selected for a more detailed study of their inhibition mechanism.

Study of the Inhibition Mechanism. Given the finding that sustained increase of 2-AG levels resulting either from repeated administration of the irreversible MAGL inhibitor 1 or by genetic deletion of the enzyme desensitizes CB₁ in the central nervous system and impairs antinociceptive effects of MAGL inhibitors,⁹ it is important to identify reversible inhibitors in order to determine whether such compounds

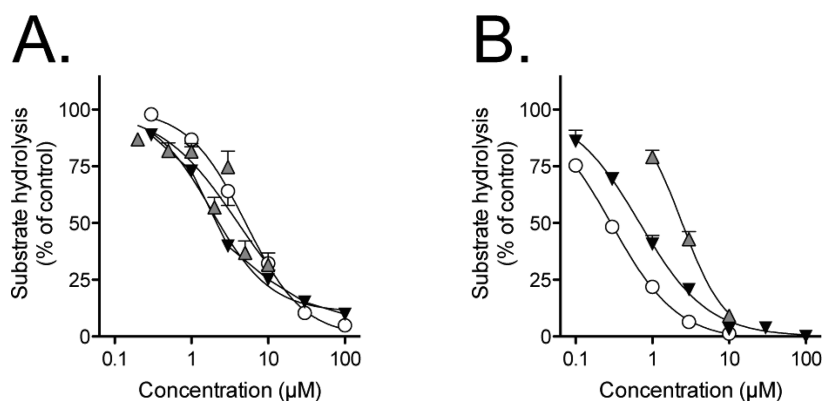


Figure 2. Concentration–response curves for compounds 8 (A) and 30 (B) (○, AEA hydrolysis; ▼, rat cytosolic 2-OG hydrolysis; ▲, hrMAGL NPA hydrolysis). Means and sem (when not enclosed by the symbol), *n* = 3–7.

avoid this problem. Therefore, we next studied the inhibition mechanism of the optimal compounds identified in these series **8** and **30**. To assess the reversible character of inhibition, we studied the effect of preincubation and dilution (Figure 3) in

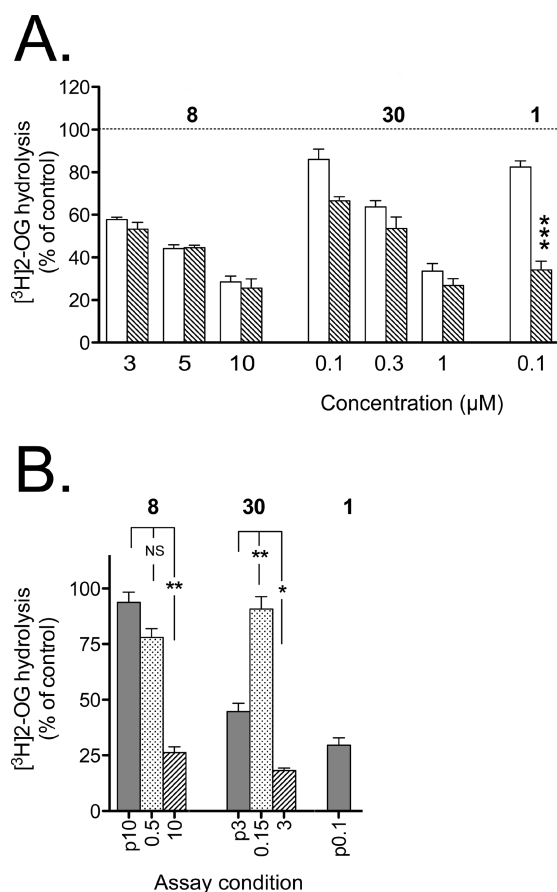


Figure 3. (A) Effect of preincubation for 0 min (white bars) or 60 min (dashed bars) of compounds **8**, **30**, and, for comparative purposes, **1** at 37 °C upon the inhibition of the hydrolysis of 2-OG. Shown are means and s.e.m., $n = 3-4$. *** $p < 0.01$ vs the corresponding non-preincubation values, two-tailed paired t test; otherwise, $p > 0.05$ (note that the significance level for 0.1 μM **30** was $p = 0.06$). (B) Assessment of the reversibility of the inhibition by **8** and **30** of rat cerebellar cytosolic 2-OG hydrolysis. Samples were preincubated for 60 min with either vehicle or the concentration shown ("p10" = preincubated with 10 μM) and then diluted 20-fold, after which substrate was added and the samples were incubated for 10 min. Following the preincubation phase, vehicle samples were either treated with vehicle or the concentrations of **8** or **30** (**1** is also included for comparison). Shown are means and s.e.m., $n = 3$, of the hydrolysis rates as percent of the vehicle controls. *, <0.05 ; **, $p < 0.01$; ^{NS}, not significant, for the comparisons between the values for the inhibitor added before dilution vs after dilution, Tukey's multiple comparison test following significant one way ANOVA for repeated measures.

the inhibitory capacity of the compounds. An irreversible inhibitor will increase its capacity to block the enzyme if preincubated previously in the presence of enzyme prior to addition of substrate and assay of activity. This is indeed the case with compound **1** (Figure 3A), a known irreversible inhibitor of MAGL.⁷ On the contrary, neither **8** nor **30** showed any significant increase in their ability to block MAGL activity after 60 min (Figure 3A). In order to further support this finding, we have carried out dilution experiments (Figure 3B).

If the compound is a freely reversible inhibitor, then the inhibition should drop upon dilution, whereas, if it is a tight-binding inhibitor, the inhibition should remain. Thus, for a fully reversible compound, the inhibition produced by preincubation with a 10 μM concentration of the compound (p10), for example, should be the same after dilution as that produced by 0.5 μM of the inhibitor added after the dilution stage. Conversely, for a tight-binding compound, the inhibition produced by p10 should be similar to that produced by 10 μM of the inhibitor added after the dilution stage, given that the compounds tested do not show time-dependent inhibition. Accordingly, derivative **8** behaves as a freely reversible inhibitor (the inhibition caused by 10 μM of the compound significantly decreases compared with the inhibition observed upon the 20-fold dilution (p10 in Figure 3B, $p < 0.01$), and no significant difference between p10 and 0.5 μM is observed. On the other hand, **30** is something in between freely reversible and tight-binding (Figure 3B), since a drop in activity is observed between a concentration of the compound of 3 μM and p3 (compatible with freely reversible) but the inhibition of p3 is significantly higher than that produced by 0.15 μM (compatible with tight binding). This latter behavior has been previously observed in other MAGL inhibitors, such as troglitazone.¹⁷ Similar results were found for AEA hydrolysis by **8** and **30** (data not shown).

Having confirmed the reversibility of both **8** and **30**, we then determined the mode of inhibition using hrMAGL expressed and purified in our laboratories (see Supporting Information for details). Our results indicate that compound **8** acts as a competitive inhibitor (Figure 4A) with a K_i value of $8 \pm 2 \mu\text{M}$ whereas inhibitor **30** is noncompetitive (Figure 4B) with a K_i value of $40 \pm 3 \mu\text{M}$. Furthermore, additional NMR experiments in the presence of hrMAGL indicated that, in fact, **8** was hydrolyzed by MAGL over time whereas **30** was unaffected during the same time interval (Figure S1 of the Supporting Information). These results are in agreement with the fact that **8** could inhibit the enzyme by acting as a competing substrate, and they also support the noncompetitive nature of **30**, which is not hydrolyzed by hrMAGL under the same experimental conditions. In order to check whether the initially proposed model was indeed compatible with these experimental results, we confirmed that both enantiomers of **8** (compounds **28** and **29**) fitted in a similar manner in the binding pocket of MAGL (Figure S2). In addition, the distance and relative orientation of the hydroxyl group of the catalytic serine and the carbonyl group of enantiomers **28** and **29** makes possible the nucleophilic attack of the serine and the subsequent hydrolysis of the substrate. Hence, this model is in agreement with the lack of stereoselectivity and with the competitive mechanism observed. On the contrary, the facts that compound **30** is not hydrolyzed under the same conditions as those for **8** (Figure S1) and that **30** behaves in a noncompetitive manner suggest that these molecules have a different mechanism of action. A reasonable explanation could be that while enantiomers **28** and **29** bind in the same pocket used by the endogenous substrate, derivative **30** inhibits MAGL activity by binding in a different site of the enzyme. Alternatively, it is also possible that **30** can bind simultaneously to 2-AG, given that the hydrophobic channel leading to the catalytic serine is quite wide. Any of these two possibilities is compatible with the fact that **30** is not hydrolyzed in the presence of enzyme as observed by NMR (Figure S1) and with the noncompetitive inhibition mechanism experimentally observed (Figure 4B) but cannot be unequiv-

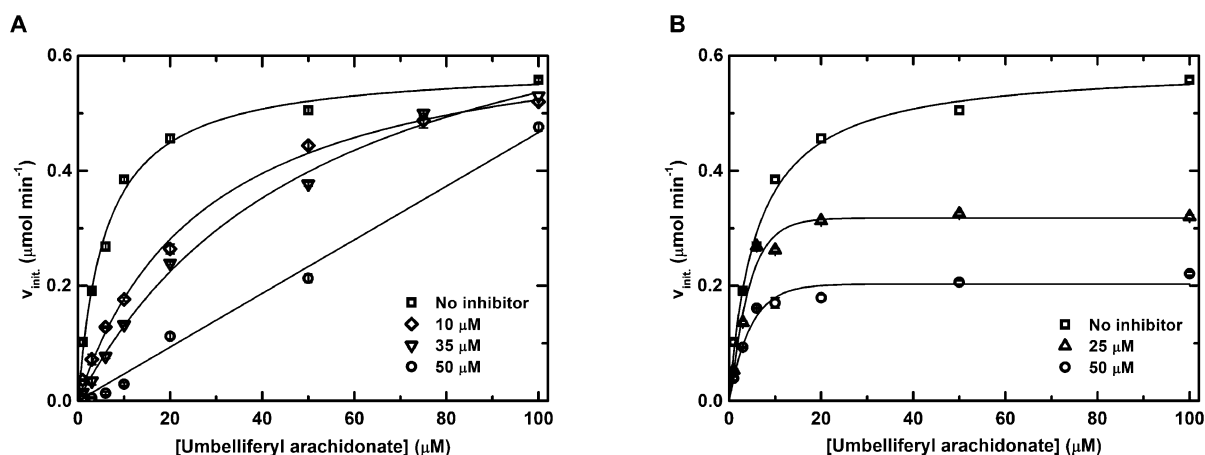


Figure 4. Inhibition of the activity of the hrMAGL: (A) competitive nature of compound **8** and (B) noncompetitive nature of derivative **30**. Shown are means \pm sem ($n = 2-3$, error bars for each point are smaller than the symbols).

ocally demonstrated with the current available structural models.

In conclusion, in this work we have developed new dual MAGL and FAAH inhibitors. Among the synthesized compounds we identified two reversible inhibitors of hrMAGL, compounds **8** and **30**, that block not only hrMAGL activity [$IC_{50}(\mathbf{8}) = 4.1 \mu\text{M}$; $IC_{50}(\mathbf{30}) = 2.4 \mu\text{M}$] but also brain monoacylglycerol hydrolysis [$IC_{50}(\mathbf{8}) = 1.8 \mu\text{M}$; $IC_{50}(\mathbf{30}) = 0.68 \mu\text{M}$]. Derivative **8** was found to inhibit MAGL by acting as a competing substrate, whereas **30** behaved as a noncompetitive inhibitor. Such compounds could open new perspectives for assessing the therapeutic potential of the time-controlled and fine-tuned modulation of 2-AG levels by means of reversible inhibition of MAGL activity.

EXPERIMENTAL SECTION

Molecular Modeling. Docking calculations have been carried out using Glide.^{14,15} Protein coordinates were downloaded from the Protein Data Bank, accession code 3JW8. Chain B, 2-methyl-pentane-2,4-diol, and water molecules (except water molecules 446 and 529) were removed. The box was centered on the centroid of residues Ala 61 and Leu 215, as in the previous work of Bertrand et al.¹³ Docking solutions were refined using MM-GBSA (molecular mechanics with generalized Born surface area), as implemented in Prime.¹⁶ Residues at a distance of 12 Å from the ligand were considered as a flexible region in the refinement.

Chemistry. Melting points (mp, uncorrected) were determined on a Stuart Scientific electrothermal apparatus for all solid compounds. Those compounds for which mp was not determined were oils. Infrared (IR) spectra were measured on a Perkin-Elmer 781, Shimadzu-8300 infrared spectrophotometer, or a Bruker Tensor 27 instrument equipped with a Specac ATR accessory of 5200–650 cm^{-1} transmission range; frequencies (ν) are expressed in cm^{-1} . Optical rotation $[\alpha]$ was measured using a Perkin-Elmer 781 polarimeter. ^1H and ^{13}C NMR spectra have been obtained at the UCM's NMR core facility and were recorded on a Varian VXR-300S, Bruker Avance 300 a.m. or Bruker 200-AC instrument at room temperature (rt) unless stated otherwise. Chemical shifts (δ) are expressed in parts per million relative to internal tetramethylsilane; coupling constants (J) are in hertz (Hz). The following abbreviations are used to describe peak patterns when appropriate: s (singlet), d (doublet), t (triplet), q (quartet), qt (quintuplet), sept (septuplet), m (multiplet), br (broad), app (apparent). For all final compounds, purity was determined either by elemental analyses or high-performance liquid chromatography coupled to mass spectrometry (HPLC-MS) and high-resolution mass spectrometry (HRMS). Elemental analyses (C, H, N) were performed on a LECO CHNS-932 apparatus at the UCM's analysis services and

were within 0.5% of the theoretical values, confirming a purity of at least 95% of all tested compounds. In the case of HPLC-MS, satisfactory chromatograms (purity >95%) were obtained. HPLC-MS analysis was performed using an Agilent 1200LC-MSD VL instrument. LC separation was achieved with an Eclipse XDB-C18 column (5 μm , 4.6 mm \times 150 mm) together with a guard column (5 μm , 4.6 mm \times 12.5 mm). The gradient mobile phases consisted of A (95:5 water/acetonitrile or water/methanol) and B (5:95 water/acetonitrile or water/methanol) with 0.1% ammonium hydroxide and 0.1% formic acid as the solvent modifiers. The gradient started at 0% B (for 5 min) and increased linearly to 100% B over the course of 20 min, with a flow rate of 0.5 mL/min, and it was followed by an isocratic gradient of 100% B for 5 min before equilibrating for 5 min at 0% B. MS analysis was performed with an electrospray ionization (ESI) source. The capillary voltage was set to 3.0 kV, and the fragmentor voltage was set at 70 eV. The drying gas temperature was 350 $^{\circ}\text{C}$, the drying gas flow was 10 L/min, and the nebulizer pressure was 20 psi. HRMS was carried out on a FTMS Bruker APEX Q IV spectrometer in ESI mode at UCM's mass spectrometry core facility. Thin-layer chromatography (TLC) was run on Merck silica gel type 60 F-254 plates. For normal pressure chromatography, Merck silica gel type (size 70–230) was used. Unless stated otherwise, the starting materials used were high-grade commercial products from Sigma-Aldrich, Acros, Fluka, Merck, or Panreac. Methylene chloride was used freshly distilled over CaH_2 . Elemental or HPLC-MS purity analyses of final compounds **4–33** and synthesis of all intermediates are described in the Supporting Information.

General Procedure for the Synthesis of Final Compounds 4–18 and 20–31. To a stirred solution of 1 equiv (100 mg) of carboxylic acid in dry dichloromethane (0.82 mL/mmol) and the appropriate alcohol (5 equiv) in dry dichloromethane (0.27 mL/mmol) in an ice bath under argon was added dropwise a solution of DCC (1 equiv) and DMAP (0.068 equiv) in dry dichloromethane (1.9 mL/mmol). The mixture was stirred for 5 min at this temperature and then removed from the cooling bath and stirred at rt (3–6 h) until no further evolution was observed by TLC. The dicyclohexylurea was filtered off, and the filtrate was washed with saturated NaHCO_3 . The organic extracts were dried over anhydrous Na_2SO_4 . Then, the solvent was evaporated under reduced pressure and the product purified by column chromatography on silica gel using the appropriate eluent.

(±)-Tetrahydro-2H-pyran-2-ylmethyl (2E)-4-(1,1'-Biphenyl-4-yl)but-2-enoate (19). To a solution of (1,1'-biphenyl-4-yl)-acetaldehyde (1.0 mmol, 1 equiv) in anhydrous toluene (12 mL/mmol) was added tetrahydro-2H-pyran-2-ylmethyl (triphenylphosphoranylidene)acetate (1 equiv). The reaction mixture was stirred at reflux for 30 min. The solvent was evaporated under reduced pressure and the product purified by column chromatography on silica gel.

General Procedure for the Synthesis of Final Compounds 32 and 33. To a solution of 1.0 mmol of the corresponding benzylated intermediates in a mixture of dry dichloromethane/absolute ethanol (3:1; 115 mL/mmol) was added Pd(OH)₂ (327 mg/mmol), and the mixture was hydrogenated in a Parr hydrogenator (hydrogen initial pressure 50 psi) during 3 h at rt. The catalyst was filtered off over Celite, and the solvent was evaporated under reduced pressure. The resulting final compounds were purified by column chromatography on silica gel.

(±)-Oxiran-2-ylmethyl (1,1'-Biphenyl-4-yl)acetate (4). Yield: 55%. R_f: 0.3 (dichloromethane). mp: 55–57 °C. IR (CH₂Cl₂, cm⁻¹): 2922, 2854, 1740, 1462, 1248, 1152, 1009, 856. ¹H NMR (CDCl₃, δ): 2.63 (dd, *J* = 4.9; 2.6 Hz, 1H, 1H oxirane); 2.82–2.86 (m, 1H, 1H oxirane); 3.19–3.27 (m, 1H, 1H oxirane); 3.72 (s, 2H, CH₂CO); 3.96 (dd, *J* = 12.3 Hz, 6.2 Hz, 1H, CH_{2a}-ox); 4.47 (dd, *J* = 12.3; 3.0 Hz, 1H, CH_{2b}-ox); 7.31–7.48 (m, 5H, 5H_{Ar}); 7.54–7.61 (m, 4H, 4H_{Ar}). ¹³C NMR (CDCl₃, δ): 40.5 (CH₂CO), 44.4 (CH₂ oxirane), 49.1 (CH oxirane), 65.1 (CH₂-ox), 126.9 (2CH_{Ar}), 127.1 (CH_{Ar}), 127.2 (2CH_{Ar}), 128.5 (2CH_{Ar}), 129.5 (2CH_{Ar}), 132.5, 140.3, 140.8 (3C_{Ar}), 171.3 (CO). Chromatography: dichloromethane. HRMS (ESI): calcd for (M + Na)⁺: 291.0997. Found: 291.0986. Anal.: (C₁₇H₁₆O₃) C, H, N.

(±)-Oxiran-2-ylmethyl 3-(1,1'-Biphenyl-4-yl)propanoate (5). Yield: 59%. R_f: 0.4 (dichloromethane). IR (CH₂Cl₂, cm⁻¹): 2925, 2856, 1737, 1520, 1289, 1158, 840, 763. ¹H NMR (CDCl₃, δ): 2.54 (dd, *J* = 4.9; 2.6 Hz, 1H, 1H oxirane); 2.65 (t, *J* = 7.4 Hz, 2H, CH₂CO); 2.75 (app t, *J* = 4.5 Hz, 1H, 1H oxirane); 2.94 (t, *J* = 7.7 Hz, 2H, ArCH₂); 3.07–3.15 (m, 1H, 1H oxirane); 3.86 (dd, *J* = 12.3; 6.3 Hz, 1H, CH_{2a}-ox); 4.35 (dd, *J* = 12.3; 3.0 Hz, 1H, CH_{2b}-ox); 7.19–7.53 (m, 9H, 9H_{Ar}). ¹³C NMR (CDCl₃, δ): 30.4, 35.5 (ArCH₂, CH₂CO), 44.5 (CH₂ oxirane), 49.2 (CH oxirane), 64.9 (CH₂-ox), 126.9 (2CH_{Ar}), 127.0 (CH_{Ar}), 127.1 (2CH_{Ar}), 128.6 (4CH_{Ar}), 139.2, 139.3, 140.8 (3C_{Ar}), 172.4 (CO). Chromatography: dichloromethane. HRMS (ESI): calcd for (M + Na)⁺: 305.1154. Found: 305.1149. HPLC-MS: >95%.

(±)-Oxiran-2-ylmethyl 4-(1,1'-Biphenyl-4-yl)butanoate (6). Yield: 41%. R_f: 0.3 (chloroform). IR (CH₂Cl₂, cm⁻¹): 2928, 2855, 2118, 1737, 1524, 1246, 1178, 1144, 846, 759. ¹H NMR (CDCl₃, δ): 1.94 (qt, *J* = 7.4 Hz, 2H, CH₂CH₂CH₂); 2.35 (t, *J* = 7.4 Hz, 2H, CH₂CO); 2.56–2.67 (m, 3H, ArCH₂, 1H oxirane); 2.77 (app t, *J* = 4.5 Hz, 1H, 1H oxirane); 3.09–3.17 (m, 1H, 1H oxirane); 3.84 (dd, *J* = 12.3; 6.4 Hz, 1H, CH_{2a}-ox); 4.36 (dd, *J* = 12.3; 3.0 Hz, 1H, CH_{2b}-ox); 7.16–7.53 (m, 9H, 9H_{Ar}). ¹³C NMR (CDCl₃, δ): 26.4 (CH₂CH₂CH₂), 33.4, 34.7 (ArCH₂, CH₂CO), 44.7 (CH₂ oxirane), 49.4 (CH oxirane), 64.9 (CH₂-ox), 127.0 (2CH_{Ar}), 127.1 (CH_{Ar}), 127.2 (2CH_{Ar}), 128.8 (2CH_{Ar}), 129.0 (2CH_{Ar}), 139.1, 140.4, 141.0 (3C_{Ar}), 173.2 (CO). Chromatography: dichloromethane. HRMS (ESI): calcd for (M + Na)⁺: 319.1310. Found: 319.1305. HPLC-MS: >95%.

(±)-Oxiran-2-ylmethyl 5-(1,1'-Biphenyl-4-yl)pentanoate (7). Yield: 56%. R_f: 0.4 (chloroform). IR (CH₂Cl₂, cm⁻¹): 2921, 2853, 1737, 1484, 1256, 1175, 758. ¹H NMR (CDCl₃, δ): 1.57–1.71 (m, 4H, (CH₂)₂CH₂CO); 2.33 (t, *J* = 7.1 Hz, 2H, CH₂CO); 2.49–2.63 (m, 3H, ArCH₂, 1H oxirane); 2.76 (app t, *J* = 4.5 Hz, 1H, 1H oxirane); 3.10–3.16 (m, 1H, 1H oxirane); 3.84 (dd, *J* = 12.3; 6.3 Hz, 1H, CH_{2a}-ox); 4.35 (dd, *J* = 12.3; 3.0 Hz, 1H, CH_{2b}-ox); 7.16–7.19 (m, 2H, 2H_{Ar}); 7.22–7.28 (m, 1H, 1H_{Ar}); 7.33–7.38 (m, 2H, 2H_{Ar}); 7.42–7.45 (m, 2H, 2H_{Ar}); 7.48–7.52 (m, 2H, 2H_{Ar}). ¹³C NMR (CDCl₃, δ): 24.5, 30.9 (2CH₂), 34.0, 35.2 (ArCH₂, CH₂CO), 44.7 (CH₂ oxirane), 49.4 (CH oxirane), 64.9 (CH₂-ox), 127.0 (2CH_{Ar}), 127.1 (CH_{Ar}), 127.3 (2CH_{Ar}), 128.7 (2CH_{Ar}), 128.8 (2CH_{Ar}), 138.8, 141.1, 141.2 (3C_{Ar}), 173.3 (CO). Chromatography: chloroform. HRMS (ESI): calcd for (M + Na)⁺: 333.1467. Found: 333.1466. HPLC-MS: >95%.

(±)-Oxiran-2-ylmethyl 6-(1,1'-Biphenyl-4-yl)hexanoate (8). Yield: 53%. R_f: 0.2 (hexane/dichloromethane, 1:9). mp: 64–65 °C. IR (CH₂Cl₂, cm⁻¹): 2923, 2854, 2119, 1737, 1485, 1257, 1174, 1013, 759. ¹H NMR (CDCl₃, δ): 1.26–1.38 (m, 2H, CH₂(CH₂)₂CO); 1.56–1.68 (m, 4H, 2CH₂); 2.30 (t, *J* = 7.5 Hz, 2H, CH₂CO); 2.56–2.61 (m, 3H, ArCH₂, 1H oxirane); 2.76 (app t, *J* = 4.5 Hz, 1H, 1H oxirane); 3.10–3.15 (m, 1H, 1H oxirane); 3.83 (dd, *J* = 12.3; 6.3 Hz, 1H, CH_{2a}-ox); 4.35 (dd, *J* = 12.3; 3.0 Hz, 1H, CH_{2b}-ox); 7.16–7.53 (m, 9H, 9H_{Ar}).

¹³C NMR (CDCl₃, δ): 24.8, 28.8, 31.1 (3CH₂), 34.0, 35.4 (ArCH₂, CH₂CO), 44.7 (CH₂ oxirane), 49.4 (CH oxirane), 64.8 (CH₂-ox), 127.0 (3CH_{Ar}), 127.1 (2CH_{Ar}), 128.7 (2CH_{Ar}), 128.8 (2CH_{Ar}), 138.7, 141.1, 141.6 (3C_{Ar}), 173.5 (CO). Chromatography: hexane/dichloromethane, 1:9. HRMS (ESI): calcd for (M + Na)⁺: 347.1623. Found: 347.1621. Anal.: (C₂₁H₂₄O₃) C, H, N.

(±)-Oxiran-2-ylmethyl 7-(1,1'-Biphenyl-4-yl)heptanoate (9). Yield: 27%. R_f: 0.3 (dichloromethane). mp: 67 °C. IR (CH₂Cl₂, cm⁻¹): 3026, 2929, 2856, 1737, 1519, 1255, 1174, 846, 760. ¹H NMR (CDCl₃, δ): 1.30 (qt, *J* = 3.6 Hz, 4H, (CH₂)₂-(CH₂)₂-CO); 1.53–1.65 (m, 4H, 2CH₂); 2.28 (t, *J* = 7.5 Hz, 2H, CH₂CO); 2.54–2.60 (m, 3H, ArCH₂, 1H oxirane); 2.76 (app t, *J* = 4.5 Hz, 1H, 1H oxirane); 3.10–3.15 (m, 1H, 1H oxirane); 3.83 (dd, *J* = 12.3; 6.3 Hz, 1H, CH_{2a}-ox); 4.34 (dd, *J* = 12.3; 3.0 Hz, 1H, CH_{2b}-ox); 7.16–7.18 (m, 2H, 2H_{Ar}); 7.21–7.27 (m, 1H, 1H_{Ar}); 7.32–7.37 (m, 2H, 2H_{Ar}); 7.42–7.45 (m, 2H, 2H_{Ar}); 7.48–7.53 (m, 2H, 2H_{Ar}). ¹³C NMR (CDCl₃, δ): 24.8, 28.9, 29.0, 31.3 (4CH₂), 34.1, 35.5 (ArCH₂, CH₂CO), 44.7 (CH₂ oxirane), 49.4 (CH oxirane), 64.8 (CH₂-ox), 127.0 (3CH_{Ar}), 127.1 (2CH_{Ar}), 128.7 (2CH_{Ar}), 128.8 (2CH_{Ar}), 138.6, 141.2, 141.8 (3C_{Ar}), 173.5 (CO). Chromatography: dichloromethane. HRMS (ESI): calcd for (M + Na)⁺: 361.1780. Found: 361.1778. Anal.: (C₂₂H₂₆O₃) C, H, N.

(±)-Tetrahydro-2H-pyran-2-ylmethyl (1,1'-Biphenyl-4-yl)acetate (10). Yield: 58%. R_f: 0.3 (chloroform). mp: 37 °C. IR (CH₂Cl₂, cm⁻¹): 2935, 2853, 1736, 1152, 1088, 1048, 1007, 752. ¹H NMR (CDCl₃, δ): 1.49–1.53 (m, 5H, 5H tetrahydropyran); 1.75–1.82 (m, 1H, 1H tetrahydropyran); 3.31–3.54 (m, 2H, 2H tetrahydropyran); 3.64 (s, 2H, CH₂CO); 3.91–4.04 (m, 3H, 1H tetrahydropyran, CH₂-tet); 7.29–7.48 (m, 5H, 5H_{Ar}); 7.52–7.61 (m, 4H, 4H_{Ar}). ¹³C NMR (CDCl₃, δ): 22.8, 25.5, 27.6 (3CH₂ tetrahydropyran), 40.6 (CH₂CO), 67.7 (CH₂-tet), 68.2 (OCH₂ tetrahydropyran), 75.2 (OCH tetrahydropyran), 126.8 (2CH_{Ar}), 127.0 (CH_{Ar}), 127.1 (2CH_{Ar}), 128.5 (2CH_{Ar}), 129.5 (2CH_{Ar}), 132.9, 139.8, 140.7 (3C_{Ar}), 171.4 (CO). Chromatography: chloroform. HRMS (ESI): calcd for (M + Na)⁺: 333.1467. Found: 333.1461. Anal.: (C₂₀H₂₂O₃) C, H, N.

(±)-Tetrahydro-2H-pyran-2-ylmethyl 3-(1,1'-Biphenyl-4-yl)propanoate (11). Yield: 49%. R_f: 0.4 (dichloromethane). mp: 45 °C. IR (CH₂Cl₂, cm⁻¹): 2926, 2851, 1735, 1175, 1089, 1049, 835, 698. ¹H NMR (CDCl₃, δ): 1.40–1.50 (m, 5H, 5H tetrahydropyran); 1.73–1.78 (m, 1H, 1H tetrahydropyran); 2.64 (t, *J* = 7.9 Hz, 2H, CH₂CO); 2.93 (t, *J* = 7.6 Hz, 2H, ArCH₂); 3.30–3.45 (m, 2H, 2H tetrahydropyran); 3.90–4.07 (m, 3H, 1H tetrahydropyran, CH₂-tet); 7.30–7.60 (m, 7H, 7H_{Ar}); 7.54–7.60 (m, 2H, 2H_{Ar}). ¹³C NMR (CDCl₃, δ): 22.9, 25.7, 27.8 (3CH₂ tetrahydropyran), 30.5, 35.6 (CH₂CO, ArCH₂), 67.5 (CH₂-tet), 68.4 (OCH₂ tetrahydropyran), 75.4 (OCH tetrahydropyran), 126.9 (2CH_{Ar}), 127.1 (CH_{Ar}), 127.2 (2CH_{Ar}), 128.7 (2CH_{Ar}), 128.8 (2CH_{Ar}), 139.2, 139.6, 140.9 (3C_{Ar}), 172.9 (CO). Chromatography: dichloromethane. HRMS (ESI): calcd for (M + Na)⁺: 347.1623. Found: 347.1632. Anal.: (C₂₁H₂₄O₃) C, H, N.

(±)-Tetrahydro-2H-pyran-2-ylmethyl 4-(1,1'-Biphenyl-4-yl)butanoate (12). Yield: 71%. R_f: 0.2 (hexane/chloroform, 1:9). mp: 51 °C. IR (CH₂Cl₂, cm⁻¹): 2938, 2852, 1734, 1179, 1089, 844, 756, 699. ¹H NMR (CDCl₃, δ): 1.40–1.49 (m, 5H, 5H tetrahydropyran); 1.78–1.82 (m, 1H, 1H tetrahydropyran); 1.92 (qt, *J* = 7.5 Hz, 2H, CH₂CH₂CH₂); 2.34 (t, *J* = 7.4 Hz, 2H, CH₂CO); 2.63 (t, *J* = 7.6 Hz, 2H, ArCH₂); 3.31–3.49 (m, 2H, 2H tetrahydropyran); 3.90–4.07 (m, 3H, 1H tetrahydropyran, CH₂-tet); 7.16–7.18 (m, 2H, 2H_{Ar}); 7.21–7.27 (m, 1H, 1H_{Ar}); 7.32–7.38 (m, 2H, 2H_{Ar}); 7.42–7.45 (m, 2H, 2H_{Ar}); 7.47–7.51 (m, 2H, 2H_{Ar}). ¹³C NMR (CDCl₃, δ): 23.0 (CH₂ tetrahydropyran), 25.8 (CH₂CH₂CH₂), 26.5, 28.0 (2CH₂ tetrahydropyran), 33.6, 34.8 (ArCH₂, CH₂CO), 67.4 (CH₂-tet), 68.4 (OCH₂ tetrahydropyran), 75.6 (OCH tetrahydropyran), 127.0 (2CH_{Ar}), 127.1 (CH_{Ar}), 127.2 (2CH_{Ar}), 128.8 (2CH_{Ar}), 129.0 (2CH_{Ar}), 139.0, 140.6, 141.1 (3C_{Ar}), 173.5 (CO). Chromatography: hexane/chloroform, 1:9. HRMS (ESI): calcd for (M + Na)⁺: 361.1780. Found: 361.1777. Anal.: (C₂₂H₂₆O₃) C, H, N.

(±)-Tetrahydro-2H-pyran-2-ylmethyl 5-(1,1'-Biphenyl-4-yl)pentanoate (13). Yield: 54%. R_f: 0.3 (dichloromethane). IR

(CH₂Cl₂, cm⁻¹): 3028, 2933, 2853, 1735, 1519, 1487, 1177, 1088, 1050, 760, 698. ¹H NMR (CDCl₃, δ): 1.35–1.50 (m, 5H, 5H tetrahydropyran); 1.61–1.68 (m, 4H, (CH₂)₂CH₂CO); 1.76–1.81 (m, 1H, 1H tetrahydropyran); 2.33 (t, *J* = 7.1 Hz, 2H, CH₂CO); 2.60 (t, *J* = 7.1 Hz, 2H, ArCH₂); 3.32–3.50 (m, 2H, 2H tetrahydropyran); 3.91–4.05 (m, 3H, 1H tetrahydropyran, CH₂-tet); 7.16–7.19 (m, 2H, 2H_{Ar}); 7.23–7.28 (m, 1H, 1H_{Ar}); 7.32–7.40 (m, 2H, 2H_{Ar}); 7.42–7.45 (m, 2H, 2H_{Ar}); 7.48–7.53 (m, 2H, 2H_{Ar}). ¹³C NMR (CDCl₃, δ): 23.0 (CH₂ tetrahydropyran), 24.6 (CH₂), 25.8, 27.9 (2CH₂ tetrahydropyran), 30.9 (CH₂), 34.1, 35.2 (ArCH₂, CH₂CO), 67.4 (CH₂-tet), 68.5 (OCH₂ tetrahydropyran), 75.5 (OCH tetrahydropyran), 127.0 (3CH_{Ar}), 127.1 (2CH_{Ar}), 128.7 (2CH_{Ar}), 128.8 (2CH_{Ar}), 138.9, 141.3, 141.7 (3C_{Ar}), 173.7 (CO). Chromatography: dichloromethane. HRMS (ESI): calcd for (M + Na)⁺: 375.1936. Found: 375.1941. HPLC-MS: >95%.

(±)-Tetrahydro-2H-pyran-2-ylmethyl 6-(1,1'-Biphenyl-4-yl)-hexanoate (14). Yield: 29%. *R*_f: 0.2 (dichloromethane). IR (CH₂Cl₂, cm⁻¹): 3029, 2929, 2854, 1733, 1453, 1272, 1180, 1089, 756, 698. ¹H NMR (CDCl₃, δ): 1.20–1.66 (m, 11H, 3CH₂, 5H tetrahydropyran); 1.77–1.80 (m, 1H, 1H tetrahydropyran); 2.29 (t, *J* = 7.5 Hz, 2H, CH₂CO); 2.58 (t, *J* = 7.7 Hz, 2H, ArCH₂); 3.32–3.48 (m, 2H, 2H tetrahydropyran); 3.90–4.04 (m, 3H, CH₂-tet, 1H tetrahydropyran); 7.15–7.18 (m, 2H, 2H_{Ar}); 7.22–7.27 (m, 1H, 1H_{Ar}); 7.32–7.40 (m, 2H, 2H_{Ar}); 7.42–7.45 (m, 2H, 2H_{Ar}); 7.48–7.60 (m, 2H, 2H_{Ar}). ¹³C NMR (CDCl₃, δ): 23.0 (CH₂ tetrahydropyran), 24.8 (CH₂), 25.8, 27.9 (2CH₂ tetrahydropyran), 28.8, 31.1 (2CH₂), 34.1, 35.4 (ArCH₂, CH₂CO), 67.4 (CH₂-tet), 68.5 (OCH₂ tetrahydropyran), 75.5 (OCH tetrahydropyran), 127.0 (3CH_{Ar}), 127.1 (2CH_{Ar}), 128.7 (2CH_{Ar}), 138.7, 141.2, 141.7 (3C_{Ar}), 173.9 (CO). Chromatography: dichloromethane. HRMS (ESI): calcd for (M + Na)⁺: 389.2093. Found: 389.2091. HPLC-MS: >95%.

(±)-Tetrahydro-2H-pyran-2-ylmethyl 7-(1,1'-Biphenyl-4-yl)-heptanoate (15). Yield: 32%. *R*_f: 0.2 (hexane/ethyl acetate, 9:1). IR (CH₂Cl₂, cm⁻¹): 3028, 2930, 2853, 1735, 1519, 1177, 1088, 760, 733. ¹H NMR (CDCl₃, δ): 1.18–1.41 (m, 6H, 3CH₂); 1.43–1.66 (m, 7H, CH₂, 5H tetrahydropyran); 1.75–1.80 (m, 1H, 1H tetrahydropyran); 2.28 (t, *J* = 7.5 Hz, 2H, CH₂CO); 2.56 (t, *J* = 7.7 Hz, 2H, ArCH₂); 3.32–3.49 (m, 2H, 2H tetrahydropyran); 3.90–4.04 (m, 3H, CH₂-tet, 1H tetrahydropyran); 7.15–7.18 (m, 2H, 2H_{Ar}); 7.21–7.27 (m, 1H, 1H_{Ar}); 7.32–7.39 (m, 2H, 2H_{Ar}); 7.41–7.45 (m, 2H, 2H_{Ar}); 7.47–7.53 (m, 2H, 2H_{Ar}). ¹³C NMR (CDCl₃, δ): 23.0 (CH₂ tetrahydropyran), 24.9 (CH₂), 25.8, 27.8 (2CH₂ tetrahydropyran), 28.9, 29.0, 31.3 (3CH₂), 34.2, 35.5 (ArCH₂, CH₂CO), 67.3 (CH₂-tet), 68.5 (OCH₂ tetrahydropyran), 75.5 (OCH tetrahydropyran), 126.9 (2CH_{Ar}), 127.0 (3CH_{Ar}), 128.7 (2CH_{Ar}), 128.8 (2CH_{Ar}), 138.6, 141.2, 141.9 (3C_{Ar}), 173.9 (CO). Chromatography: hexane/ethyl acetate, 9:1. HRMS (ESI): calcd for (M + Na)⁺: 403.2249. Found: 403.2253. HPLC-MS: >95%.

(±)-Oxiran-2-ylmethyl (2E)-3-(1,1'-Biphenyl-4-yl)acrilate (16). Yield: 41%. *R*_f: 0.3 (dichloromethane). mp: 99 °C. IR (CH₂Cl₂, cm⁻¹): 2925, 2852, 1713, 1636, 1450, 1349, 1266, 1187, 1177, 985, 852, 768. ¹H NMR (CDCl₃, δ): 2.72 (dd, *J* = 4.9; 2.6 Hz, 1H, 1H oxirane); 2.88–2.92 (m, 1H, 1H oxirane); 3.27–3.35 (m, 1H, 1H oxirane); 4.06 (dd, *J* = 12.3; 6.3 Hz, 1H, CH_{2a}-ox); 4.57 (dd, *J* = 12.3; 3.0 Hz, 1H, CH_{2b}-ox); 6.51 (d, *J* = 16.0 Hz, 1H, CH-CO); 7.34–7.51 (m, 3H, 3H_{Ar}); 7.59–7.67 (m, 6H, 6H_{Ar}); 7.77 (d, *J* = 16.0 Hz, 1H, ArCH). ¹³C NMR (CDCl₃, δ): 44.8 (CH₂ oxirane), 49.5 (CH oxirane), 65.1 (CH₂-ox), 117.2 (CHCO), 127.1 (2CH_{Ar}), 127.6 (CH_{Ar}), 127.9 (2CH_{Ar}), 128.7 (2CH_{Ar}), 128.9 (2CH_{Ar}), 133.2, 140.1, 143.3 (3C_{Ar}), 145.2 (ArCH), 166.7 (CO). Chromatography: dichloromethane. HRMS (ESI): calcd for (M + Na)⁺: 303.0997. Found: 303.0998. Anal.: (C₁₈H₁₆O₃) C, H, N.

(±)-Tetrahydro-2H-pyran-2-ylmethyl (2E)-3-(1,1'-Biphenyl-4-yl)acrilate (17). Yield: 60%. *R*_f: 0.2 (dichloromethane). mp: 113–115 °C. IR (CH₂Cl₂, cm⁻¹): 2940, 2850, 1712, 1636, 1317, 1175, 1085, 1048, 867, 801. ¹H NMR (CDCl₃, δ): 1.30–1.59 (m, 5H, 5H tetrahydropyran); 1.79–1.90 (m, 1H, 1H tetrahydropyran); 3.35–3.46 (m, 1H, 1H tetrahydropyran); 3.49–3.57 (m, 1H, 1H tetrahydropyran); 4.09–4.22 (m, 3H, 1H tetrahydropyran, CH₂-tet); 6.48 (d, *J* = 16.0 Hz, 1H, CHCO); 7.26–7.43 (m, 3H, 3H_{Ar}); 7.52–

7.57 (m, 6H, 6H_{Ar}); 7.68 (d, *J* = 16.0 Hz, 1H, ArCH). ¹³C NMR (CDCl₃, δ): 23.0, 25.8, 27.9 (3CH₂ tetrahydropyran), 67.6 (CH₂-tet), 68.5 (OCH₂ tetrahydropyran), 75.6 (OCH tetrahydropyran), 117.8 (CHCO), 127.0 (2CH_{Ar}), 127.5 (2CH_{Ar}), 127.8 (CH_{Ar}), 128.6 (2CH_{Ar}), 128.9 (2CH_{Ar}), 133.4, 140.2, 143.1 (3C_{Ar}), 144.6 (ArCH), 167.1 (CO). Chromatography: dichloromethane. HRMS (ESI): calcd for (M + Na)⁺: 345.1467. Found: 345.1469. Anal.: (C₂₁H₂₂O₃) C, H, N.

(±)-Tetrahydro-2H-pyran-2-ylmethyl (3E)-4-(1,1'-Biphenyl-4-yl)but-3-enoate (18). Yield: 69%. *R*_f: 0.2 (hexane/dichloromethane, 2:8). mp: 92–94 °C. IR (CH₂Cl₂, cm⁻¹): 3032, 2938, 2852, 1734, 1262, 1162, 1090, 759. ¹H NMR (CDCl₃, δ): 1.22–1.56 (m, 5H, 5H tetrahydropyran); 1.77–1.82 (m, 1H, 1H tetrahydropyran); 3.25 (dd, *J* = 6.9; 1.1 Hz, 2H, CH₂CO); 3.34–3.47 (m, 2H, 2H tetrahydropyran), 3.98–4.09 (m, 3H, CH₂-tet, 1H tetrahydropyran); 6.28 (dt, *J* = 15.9; 7.0 Hz, 1H, CHCH₂); 6.46 (d, *J* = 15.9 Hz, 1H, ArCH), 7.26–7.38 (m, 5H, 5H_{Ar}), 7.46–7.54 (m, 4H, 4H_{Ar}). ¹³C NMR (CDCl₃, δ): 23.0, 25.8, 27.9 (3CH₂ tetrahydropyran), 38.3 (CH₂CO), 67.8 (CH₂-tet), 68.5 (OCH₂ tetrahydropyran), 75.4 (OCH tetrahydropyran), 121.9 (CHCH₂), 126.7 (2CH_{Ar}), 126.9 (2CH_{Ar}), 127.2 (2CH_{Ar}), 127.3 (CH_{Ar}), 128.8 (2CH_{Ar}), 133.0 (ArCH), 136.3, 140.3, 140.7 (3C_{Ar}), 171.6 (CO). Chromatography: hexane/dichloromethane, 2:8. HRMS (ESI): calcd for (M + Na)⁺: 359.1623. Found: 359.1622. Anal.: (C₂₂H₂₄O₃) C, H, N.

(±)-Tetrahydro-2H-pyran-2-ylmethyl (2E)-4-(1,1'-Biphenyl-4-yl)but-2-enoate (19). Yield: 67%. *R*_f: 0.2 (hexane/dichloromethane, 2:8). mp: 71 °C. IR (CH₂Cl₂, cm⁻¹): 3029, 2936, 2850, 1718, 1653, 1269, 1087, 763. ¹H NMR (CDCl₃, δ): 1.18–1.55 (m, 5H, 5H tetrahydropyran); 1.76–1.81 (m, 1H, 1H tetrahydropyran); 3.32–3.53 (m, 4H, ArCH₂, 2H tetrahydropyran); 3.91–4.10 (m, 3H, CH₂-tet, 1H tetrahydropyran); 5.83 (dt, *J* = 15.6; 1.6 Hz, 1H, CH₂CH=CH); 7.10 (dt, *J* = 15.6; 6.7 Hz, 1H, CHCO); 7.19–7.39 (m, 5H, 5H_{Ar}); 7.46–7.53 (m, 4H, 4H_{Ar}). ¹³C NMR (CDCl₃, δ): 23.0, 25.8, 27.9 (3CH₂ tetrahydropyran), 38.1 (ArCH₂), 67.4 (CH₂-tet), 68.4 (OCH₂ tetrahydropyran), 75.5 (OCH tetrahydropyran), 122.2 (CH₂CH=CH), 127.1 (2CH_{Ar}), 127.2 (CH_{Ar}), 127.5 (2CH_{Ar}), 128.8 (2CH_{Ar}), 129.3 (2CH_{Ar}), 136.7, 139.7, 140.9 (3C_{Ar}), 147.7 (CHCO), 166.5 (CO). Chromatography: hexane/dichloromethane, 2:8. HRMS (ESI): calcd for (M + Na)⁺: 359.1623. Found: 359.1616. Anal.: (C₂₂H₂₄O₃) C, H, N.

(±)-Oxiran-2-ylmethyl (4-Benzylphenyl)acetate (20). Yield: 71%. *R*_f: 0.3 (dichloromethane). IR (CH₂Cl₂, cm⁻¹): 2922, 2853, 1738, 1147, 1011, 854. ¹H NMR (CDCl₃, δ): 2.61 (dd, *J* = 4.8; 2.6 Hz, 1H, 1H oxirane), 2.80–2.84 (m, 1H, 1H oxirane), 3.16–3.24 (m, 1H, 1H oxirane), 3.64 (s, 2H, ArCH₂CO), 3.89–3.97 (m, 3H, ArCH₂Ar, CH_{2a}-ox), 4.43 (dd, *J* = 12.3; 3.0 Hz, 1H, CH_{2b}-ox), 7.05–7.25 (m, 9H, 9H_{Ar}). ¹³C NMR (CDCl₃, δ): 40.6 (ArCH₂CO), 41.5 (ArCH₂Ar), 44.6 (OCH₂ oxirane), 49.3 (OCH oxirane), 65.2 (CH₂-ox), 126.1 (CH_{Ar}), 128.4 (2CH_{Ar}), 128.9 (2CH_{Ar}), 129.2 (2CH_{Ar}), 129.4 (2CH_{Ar}), 131.5, 140.1, 141.5 (3C_{Ar}), 171.5 (CO). Chromatography: dichloromethane. HRMS (ESI): calcd for (M + Na)⁺: 305.1154. Found: 305.1150. HPLC-MS: >95%.

(±)-Oxiran-2-ylmethyl 3-(4-Benzylphenyl)propanoate (21). Yield: 75%. *R*_f: 0.2 (hexane/dichloromethane, 3:7). IR (CH₂Cl₂, cm⁻¹): 3020, 2926, 2855, 1737, 1156, 907, 848. ¹H NMR (CDCl₃, δ): 2.58–2.70 (m, 3H, 1H oxirane, CH₂CO); 2.79–2.83 (m, 1H, 1H oxirane); 2.90–2.98 (m, 2H, ArCH₂CH₂); 3.13–3.21 (m, 1H, 1H oxirane); 3.84–3.95 (m, 3H, ArCH₂Ar, CH_{2a}-ox); 4.40 (dd, *J* = 12.3; 3.1 Hz, 1H, CH_{2b}-ox); 7.07–7.35 (m, 9H, 9H_{Ar}). ¹³C NMR (CDCl₃, δ): 30.5, 35.7 (CH₂CO, ArCH₂CH₂), 41.6 (ArCH₂Ar), 44.7 (CH₂ oxirane), 49.3 (CH oxirane), 65.0 (CH₂-ox), 126.1 (CH_{Ar}), 128.4 (2CH_{Ar}), 128.5 (2CH_{Ar}), 128.9 (2CH_{Ar}), 129.1 (2CH_{Ar}), 138.0, 139.2, 141.2 (3C_{Ar}), 172.6 (CO). Chromatography: hexane/dichloromethane, 3:7. HRMS (ESI): calcd for (M + Na)⁺: 319.1310. Found: 319.1302. HPLC-MS: >95%.

(±)-Oxiran-2-ylmethyl 4-(4-Benzylphenyl)butanoate (22). Yield: 76%. *R*_f: 0.3 (dichloromethane). IR (CH₂Cl₂, cm⁻¹): 3019, 2924, 2854, 1737, 1504, 1449, 1177, 1143, 850. ¹H NMR (CDCl₃, δ): 1.85 (qt, *J* = 7.3 Hz, 2H, CH₂CH₂CH₂); 2.27 (t, *J* = 7.5 Hz, 2H, CH₂CO); 2.49–2.56 (m, 3H, ArCH₂CH₂, 1H oxirane); 2.74 (app t, *J*

= 6.0 Hz, 1H, 1H oxirane); 3.05–3.13 (m, 1H, 1H oxirane); 3.74–3.89 (m, 3H, ArCH₂Ar, CH_{2a}-ox); 4.30 (dd, *J* = 12.3; 3.0 Hz, 1H, CH_{2b}-ox); 7.07–7.23 (m, 9H, 9H_{Ar}). ¹³C NMR (CDCl₃, δ): 26.4 (CH₂CH₂CH₂), 33.4, 34.7 (CH₂CO, ArCH₂), 41.5 (ArCH₂Ar), 44.6 (CH₂ oxirane), 49.3 (CH oxirane), 64.8 (CH₂-ox), 126.0 (CH_{Ar}), 128.4 (2CH_{Ar}), 128.6 (2CH_{Ar}), 128.8 (2CH_{Ar}), 128.9 (2CH_{Ar}), 138.9, 139.0, 141.3 (3C_{Ar}), 173.2 (CO). Chromatography: dichloromethane. HRMS (ESI): calcd for (M + Na)⁺: 333.1467. Found: 333.1461. HPLC-MS: >95%.

(±)-Oxiran-2-ylmethyl 4-(2-Phenylethyl)benzoate (23). Yield: 75%. *R*_f: 0.3 (dichloromethane). IR (CH₂Cl₂, cm⁻¹): 2921, 2853, 1720, 1458, 1179, 1106, 843. ¹H NMR (CDCl₃, δ): 2.65 (dd, *J* = 4.8; 2.6 Hz, 1H, 1H oxirane), 2.79–2.94 (m, 5H, 1H oxirane, Ar(CH₂)₂Ar); 3.22–3.30 (m, 1H, 1H oxirane); 4.08 (dd, *J* = 12.3; 6.2 Hz, 1H, CH_{2a}-ox); 4.57 (dd, *J* = 12.3; 3.0 Hz, 1H, CH_{2b}-ox); 7.05–7.23 (m, 7H, 7H_{Ar}); 7.89 (d, *J* = 8.2 Hz, 2H, 2H_{Ar}). ¹³C NMR (CDCl₃, δ): 37.3, 37.7 (2CH₂Ar), 44.6 (CH₂ oxirane), 49.4 (CH oxirane), 65.1 (CH₂-ox), 125.9 (CH_{Ar}), 127.3 (C_{Ar}), 128.2 (2CH_{Ar}), 128.3 (2CH_{Ar}), 128.5 (2CH_{Ar}), 129.7 (2CH_{Ar}), 140.9, 147.4 (2C_{Ar}), 166.1 (CO). Chromatography: dichloromethane. HRMS (ESI): calcd for (M + Na)⁺: 305.1154. Found: 305.1146. HPLC-MS: >95%.

(±)-Tetrahydro-2H-pyran-2-ylmethyl (4-Benzylphenyl)acetate (24). Yield: 69%. *R*_f: 0.2 (chloroform). mp: 65 °C. IR (CH₂Cl₂, cm⁻¹): 3026, 2937, 2850, 1736, 1147, 1089, 1012. ¹H NMR (CDCl₃, δ): 1.21–1.56 (m, 5H, 5H tetrahydropyran); 1.81–1.86 (m, 1H, 1H tetrahydropyran); 3.36–3.58 (m, 2H, 2H tetrahydropyran); 3.64 (s, 2H, ArCH₂CO); 3.96 (s, 2H, ArCH₂Ar); 3.98–4.09 (m, 3H, CH₂-tet, 1H tetrahydropyran); 7.12–7.33 (m, 9H, 9H_{Ar}). ¹³C NMR (CDCl₃, δ): 23.0, 25.8, 27.8 (3CH₂ tetrahydropyran), 40.8 (ArCH₂CO), 41.6 (ArCH₂Ar), 67.8 (CH₂-tet), 68.4 (OCH₂ tetrahydropyran), 75.4 (OCH tetrahydropyran), 126.1 (CH_{Ar}), 128.5 (2CH_{Ar}), 128.9 (2CH_{Ar}), 129.1 (2CH_{Ar}), 129.4 (2CH_{Ar}), 131.8, 139.9, 141.1 (3C_{Ar}), 171.8 (CO). Chromatography: chloroform. HRMS (ESI): calcd for (M + Na)⁺: 347.1623. Found: 347.1626. Anal.: (C₂₁H₂₄O₃) C, H, N.

(±)-Tetrahydro-2H-pyran-2-ylmethyl 3-(4-Benzylphenyl)propanoate (25). Yield: 76%. *R*_f: 0.2 (hexane/dichloromethane, 2:8). IR (CH₂Cl₂, cm⁻¹): 3023, 2925, 2852, 1735, 1447, 1174, 1090, 855. ¹H NMR (CDCl₃, δ): 1.26–1.61 (m, 5H, 5H tetrahydropyran); 1.81–1.86 (m, 1H, 1H tetrahydropyran); 2.62–2.70 (m, 2H, CH₂CO); 2.89–2.96 (m, 2H, ArCH₂CH₂); 3.36–3.53 (m, 2H, 2H tetrahydropyran); 3.95–4.13 (m, 5H, ArCH₂Ar, 1H tetrahydropyran, CH₂-tet); 7.12–7.35 (m, 9H, 9H_{Ar}). ¹³C NMR (CDCl₃, δ): 23.0, 25.8, 27.8 (3CH₂ tetrahydropyran), 30.5, 35.8 (CH₂CO, ArCH₂CH₂), 41.6 (ArCH₂Ar), 67.5 (CH₂-tet), 68.4 (OCH₂ tetrahydropyran), 75.5 (OCH tetrahydropyran), 126.1 (CH_{Ar}), 128.4 (2CH_{Ar}), 128.5 (2CH_{Ar}), 128.9 (2CH_{Ar}), 129.0 (2CH_{Ar}), 138.2, 139.1, 141.2 (3C_{Ar}), 173.0 (CO). Chromatography: hexane/dichloromethane, 2:8. HRMS (ESI): calcd for (M + Na)⁺: 361.1780. Found: 361.1769. HPLC-MS: >95%.

(±)-Tetrahydro-2H-pyran-2-ylmethyl 4-(4-Benzylphenyl)butanoate (26). Yield: 75%. *R*_f: 0.2 (hexane/ethyl acetate, 8:2). IR (CH₂Cl₂, cm⁻¹): 3023, 2938, 2851, 1734, 1447, 1089, 772. ¹H NMR (CDCl₃, δ): 1.23–1.59 (m, 5H, 5H tetrahydropyran); 1.81–1.96 (m, 3H, 1H tetrahydropyran, CH₂CH₂CH₂); 2.34 (t, *J* = 7.4 Hz, 2H, CH₂CO); 2.58 (t, *J* = 7.6 Hz, 2H, ArCH₂CH₂); 3.36–3.54 (m, 2H, 2H tetrahydropyran); 3.89–4.08 (m, 5H, 1H tetrahydropyran, CH₂-tet, ArCH₂Ar); 7.07–7.28 (m, 9H, 9H_{Ar}). ¹³C NMR (CDCl₃, δ): 23.0 (CH₂ tetrahydropyran), 25.8 (CH₂), 26.6, 27.9 (2CH₂ tetrahydropyran), 33.6, 34.7 (CH₂CO, ArCH₂CH₂), 41.6 (ArCH₂Ar), 67.4 (CH₂-tet), 68.4 (OCH₂ tetrahydropyran), 75.5 (OCH tetrahydropyran), 126.0 (CH_{Ar}), 128.5 (2CH_{Ar}), 128.6 (2CH_{Ar}), 128.9 (4CH_{Ar}), 138.8, 139.2, 141.3 (3C_{Ar}), 173.6 (CO). Chromatography: hexane/ethyl acetate, 8:2. HRMS (ESI): calcd for (M + Na)⁺: 375.1936. Found: 375.1925. HPLC-MS: >95%.

(±)-Tetrahydro-2H-pyran-2-ylmethyl 4-(2-Phenylethyl)benzoate (27). Yield: 74%. *R*_f: 0.2 (dichloromethane). IR (CH₂Cl₂, cm⁻¹): 3029, 2933, 2853, 1718, 1091. ¹H NMR (CDCl₃, δ): 1.37–1.61 (m, 5H, 5H tetrahydropyran); 1.81–1.84 (m, 1H, 1H tetrahydropyran); 2.79–2.96 (m, 4H, Ar(CH₂)₂Ar); 3.33–3.46 (m, 1H, 1H

tetrahydropyran); 3.55–3.66 (m, 1H, 1H tetrahydropyran); 3.93–4.13 (m, 1H, 1H tetrahydropyran); 4.19–4.28 (m, 2H, CH₂-tet); 7.05–7.25 (m, 7H, 7H_{Ar}); 7.90 (dd, *J* = 6.6; 1.7 Hz, 2H, 2H_{Ar}). ¹³C NMR (CDCl₃, δ): 22.9, 25.7, 28.0 (3CH₂ tetrahydropyran), 37.3, 37.7 (2CH₂Ar), 67.6 (CH₂-tet), 68.3 (OCH₂ tetrahydropyran), 75.4 (OCH tetrahydropyran), 125.9 (CH_{Ar}), 127.8 (C_{Ar}), 128.2 (2CH_{Ar}), 128.3 (2CH_{Ar}), 128.4 (2CH_{Ar}), 129.7 (2CH_{Ar}), 141.0, 147.0 (2C_{Ar}), 166.4 (CO). Chromatography: dichloromethane. HRMS (ESI): calcd for (M + Na)⁺: 347.1623. Found: 347.1617. HPLC-MS: >95%.

(2R)-(-)-Oxiran-2-ylmethyl 6-(1,1'-Biphenyl-4-yl)hexanoate (28). Data of 28 were identical to those recorded for the racemic material 8 except for the optical rotation. 28: [α]_D²⁰ -15.5 (*c* = 1.9, ethanol). Anal.: (C₂₁H₂₄O₃) C, H, N.

(2S)-(+)-Oxiran-2-ylmethyl 6-(1,1'-Biphenyl-4-yl)hexanoate (29). Data of 29 were identical to those recorded for the racemic material 8 except for the optical rotation. 29: [α]_D²⁰ +16.3 (*c* = 1.9, ethanol). Anal.: (C₂₁H₂₄O₃) C, H, N.

(2R)-(-)-Oxiran-2-ylmethyl(4-benzylphenyl)acetate (30). Data of 30 were identical to those recorded for the racemic material 20 except for the optical rotation. 30: [α]_D²⁰ -9.1 (*c* = 1.5, ethanol). HPLC-MS: >95%.

(2S)-(+)-Oxiran-2-ylmethyl(4-benzylphenyl)acetate (31). Data of 31 were identical to those recorded for the racemic material 20 except for the optical rotation. 31: [α]_D²⁰ +9.0 (*c* = 1.5, ethanol). HPLC-MS: >95%.

2-Hydroxy-1-(hydroxymethyl)ethyl 6-(1,1'-biphenyl-4-yl)hexanoate (32). Yield: 28%. *R*_f: 0.1 (dichloromethane/ethanol, 9:6:0.4). IR (CH₂Cl₂, cm⁻¹): 3369, 2924, 2855, 1735, 1176, 744. ¹H NMR (CDCl₃, δ): 1.35–1.45 (m, 2H, CH₂(CH₂)₂CO); 1.62–1.74 (m, 4H, 2CH₂); 2.36 (t, *J* = 7.5 Hz, 2H, CH₂CO); 2.65 (t, *J* = 7.6 Hz, 2H, ArCH₂); 3.54–3.70 (m, 2H, 2CH₂OH); 3.80–3.94 (m, 1H, CHO); 4.11–4.22 (m, 2H, 2CH₂OH); 7.22–7.59 (m, 9H, 9H_{Ar}). ¹³C NMR (CDCl₃, δ): 24.8, 28.7, 31.0 (3CH₂), 34.1, 35.3 (ArCH₂, CH₂CO), 63.4, 65.2 (2CH₂OH), 70.3 (CH), 127.0 (2CH_{Ar}), 127.1 (3CH_{Ar}), 128.7 (2CH_{Ar}), 128.8 (2CH_{Ar}), 138.7, 141.1, 141.6 (3C_{Ar}), 174.2 (CO). Chromatography: dichloromethane/ethanol (9:6:0.4). HRMS (ESI): calcd for (M + Na)⁺: 365.1729. Found: 365.1709. HPLC-MS: > 95%.

2-Hydroxy-1-(hydroxymethyl)ethyl (4-Benzylphenyl)acetate (33). Yield: 70%. *R*_f: 0.3 (dichloromethane/ethanol, 9:7:0.3). mp: 82 °C. IR (CH₂Cl₂, cm⁻¹): 3404, 2924, 1732, 1157, 726, 699. ¹H NMR (CDCl₃, δ): 2.15 (br s, 2H, 2OH), 3.51–3.93 (m, 5H, 2CH₂OH, CH₂CO, CH), 3.98 (s, 2H, ArCH₂Ar), 4.13–4.24 (m, 2H, 2CH₂OH), 7.15–7.28 (m, 9H, 9H_{Ar}). ¹³C NMR (CDCl₃, δ): 41.2 (CH₂CO), 41.9 (ArCH₂Ar), 63.6, 66.1 (2CH₂OH), 70.5 (CH), 126.5 (CH_{Ar}), 128.9 (2CH_{Ar}), 129.3 (2CH_{Ar}), 129.6 (2CH_{Ar}), 129.7 (2CH_{Ar}), 131.7, 140.7, 141.3 (3C_{Ar}), 172.5 (CO). Chromatography: dichloromethane/ethanol, 9:8:0.2. HRMS (ESI): calcd for (M + Na)⁺: 300.1362. Found: 300.1365. Anal.: (C₁₈H₂₀O₄) C, H, N.

Enzyme Inhibition Assays in Brain Fractions. All final compounds were tested for their ability to inhibit 2-OG and AEA hydrolysis using a substrate concentration of 0.5 μM and the assay procedures described previously.¹⁹ FAAH and MAGL assays were undertaken using membrane and cytosolic fractions of rat cerebella. Briefly, cerebella that had been obtained previously and stored frozen were thawed and homogenized in 0.32 M sucrose containing 50 mM sodium phosphate, pH 8.0. Following homogenization, the samples were centrifuged at 100000g for 60 min at 4 °C, and the supernatants ("cytosolic fractions") were collected. The pellets were resuspended in 50 mM sodium phosphate, pH 8.0 ("membrane fractions"), and the fractions were stored frozen in aliquots until they were used for assay. Protein concentrations for the assays were set so that the initial velocities were always measured, with the fractions being diluted with 10 mM Tris-HCl, 1 mM ethylenediaminetetraacetic acid (EDTA), pH 7.2. Each assay consisted of the fraction to be tested, test compound, and substrate ([³H]-2-OG or [³H]-AEA labeled in its glycerol or ethanolamine moiety, respectively, final concentration 0.5 μM). The radiolabeled substrates were obtained from American Radiolabeled Chemicals, St. Louis, MO, USA. The substrate solution contained fatty acid-free bovine serum albumin (BSA), to give an assay concentration

of 0.125% w/v. After incubation, usually for 10 min at 37 °C, reactions were stopped by the addition of 400 μ L of active charcoal mixture (80 μ L of charcoal + 320 μ L of 0.5 M HCl). After vortex mixing and phase separation, aliquots (200 μ L) of the aqueous phase were taken and tritium content was determined by liquid scintillation spectrometry with quench collection. Blanks were prepared in the same manner but without an enzyme source. Results were expressed as percent of the activity of controls containing the same volume of solvent carrier.

hrMAGL Inhibition Assay. The method of Muccioli et al.¹⁸ was modified¹⁷ using a 96-well microtiter plate (100 mL total volume). Clear lysates of human recombinant his tagged MAGL (Cayman Chemical Co., Ann Arbor, MI, USA) in 10 mM Tris-HCl, 1 mM EDTA, pH 7.4 (added volume 70 μ L) were added to wells containing test compounds (3 μ L in vehicle) or vehicle alone. Buffer (7 μ L) was added to each well to make up the volume. To start the hydrolysis reactions, 4-nitrophenyl acetate (NPA, 20 μ L, final concentration of 0.25 mM, unless otherwise shown) was added rapidly. The samples were incubated at rt, and the absorbance was measured at 405 nm after 0 min (to rule out effects of the compounds *per se* on the absorbance) and thereafter at two 20 min intervals using a ThermoMax Microplate Reader (ThermoMax Kinetic Microplate Reader, Molecular Devices, Sunnyvale, CA, USA). The 20 min time point was used here and the data expressed as percent of vehicle control after subtraction of blank values (wells with buffer in place of enzyme).

Enzymatic Activity for Kinetic Studies. Enzymatic activity was assayed as previously described²⁰ using umbelliferyl arachidonate from Cayman Chemical Co. (Ann Arbor, MI) as substrate dissolved in dimethylsulfoxide. The fluorescence of the product 7-hydroxycoumarin released by the hydrolysis was measured with excitation and emission wavelengths of 355 and 460 nm, respectively. Fluorescence measurements were carried out in a Perkin-Elmer luminescence spectrophotometer LS50B. Excitation and emission bandwidths were 2.5 and 10 nm, respectively. The fluorescence cell (1 cm \times 0.5 cm) was mounted on a thermostatted holder. All fluorescence measurements were collected at a constant temperature of 37 °C. The reaction mixture was prepared as follows—50 μ g of MAGL protein expressed and purified as described in the Supporting Information—and the desired amount of substrate was added to 1.0 mL of buffer (50 mM Na-HEPES, pH 8.2, and 1 mM EDTA), and the reaction was followed for 2.5 min. Initial velocities were used to calculate the kinetic constants K_m and k_{cat} . The inhibition constants were calculated by performing the kinetic measurements in the presence of different amounts of the inhibitors. All constants (K_m , k_{cat} , and K_i) were calculated with the program GraphPad Prism (version 5) using the global nonlinear regression option.

■ ASSOCIATED CONTENT

■ Supporting Information

Full synthetic procedures; analytical and spectral characterization data for all intermediates; HPLC-MS and elemental analyses for all final compounds; molecular biology methods for MAGL cloning; expression and purification; NMR spectra of compounds **8** and **30** in the presence of hrMAGL over time; and computational models of the complex between the enantiomers of compound **8** (derivatives **28** and **29**). This material is available free of charge via the Internet at <http://pubs.acs.org>.

■ AUTHOR INFORMATION

Corresponding Author

*Phone: +34 913944239. Fax: +34 913944103. E-mail: mluzlr@quim.ucm.es.

■ ACKNOWLEDGMENTS

The authors are indebted to Eva Hallin and Britt Jacobsson for excellent technical assistance. This work has been supported by grants from the Spanish Ministerio de Ciencia e Innovación

(MICINN, SAF-2010/22198-C02-01, M.L.L.-R.) and from the Comunidad Autónoma de Madrid (S2010/BMD-2353, M.L.L.-R.), the Swedish Science Research Council (Grant 12158, medicine, to C.J.F.) and by the Research Funds of the Medical Faculty, Umeå University (C.J.F.). The authors thank MICINN and European Social Fund for predoctoral (J.A.C.) and Ramón y Cajal grants (S.O.-G. and A.C.).

■ ABBREVIATIONS USED

ABHD-6, α/β hydrolase-6; ABHD-12, α/β hydrolase-12; AEA, *N*-arachidonylethanolamine, anandamide; 2-AG, 2-arachidonoylglycerol; (e)CB, (endo)cannabinoid; FAAH, fatty acid amide hydrolase; hrMAGL, human recombinant MAGL; MAGL, monoacylglycerol lipase; NPA, 4-nitrophenyl acetate; 2-OG, 2-oleoylglycerol; SAR, structure–activity relationship

■ REFERENCES

- (1) Pacher, P.; B atkai, S.; Kunos, G. The endocannabinoid system as an emerging target of pharmacotherapy. *Pharmacol. Rev.* **2006**, *58*, 389–462.
- (2) Pertwee, R. G.; Howlett, A. C.; Abood, M. E.; Alexander, S. P. H.; Di Marzo, V.; Elphick, M. R.; Greasley, P. J.; Hansen, H. S.; Kunos, G. International Union of Basic and Clinical Pharmacology. LXXIX. Cannabinoid receptors and their ligands: beyond CB₁ and CB₂. *Pharmacol. Rev.* **2010**, *62*, 588–631.
- (3) Long, J. Z.; Nomura, D. K.; Vann, R. E.; Walentiny, D. M.; Booker, L.; Jin, X.; Burston, J. J.; Sim-Selley, L. J.; Lichtman, A. H.; Wiley, J. L.; Cravatt, B. F. Dual blockade of FAAH and MAGL identifies behavioral processes regulated by endocannabinoid crosstalk in vivo. *Proc. Natl. Acad. Sci. U.S.A.* **2009**, *106*, 20270–20275.
- (4) McKinney, M. K.; Cravatt, B. F. Structure and function of fatty acid amide hydrolase. *Annu. Rev. Biochem.* **2005**, *74*, 411–432.
- (5) Blankman, J. L.; Simon, G. M.; Cravatt, B. F. A comprehensive profile of brain enzymes that hydrolyze the endocannabinoid 2-arachidonoylglycerol. *Chem. Biol.* **2007**, *14*, 1347–1356.
- (6) Seierstad, M.; Breitenbucher, J. Discovery and development of fatty acid amide hydrolase (FAAH) inhibitors. *J. Med. Chem.* **2008**, *51*, 7327–7343.
- (7) Long, J. Z.; Li, W.; Booker, L.; Burston, J. J.; Kinsey, S. G.; Schlosburg, J. E.; Pav on, F. J.; Serrano, A. M.; Selley, D. E.; Parsons, L. H.; Lichtman, A. H.; Cravatt, B. F. Selective blockade of 2-arachidonoylglycerol hydrolysis produces cannabinoid behavioral effects. *Nat. Chem. Biol.* **2009**, *5*, 37–44.
- (8) Kinsey, S. G.; Long, J. Z.; O’Neal, S. T.; Abdullah, R. A.; Poklis, J. L.; Boger, D. L.; Cravatt, B. F.; Lichtman, A. H. Blockade of endocannabinoid-degrading enzymes attenuates neuropathic pain. *J. Pharmacol. Exp. Ther.* **2009**, *330*, 902–910.
- (9) Schlosburg, J. E.; Blankman, J. L.; Long, J. Z.; Nomura, D. K.; Pan, B.; Kinsey, S. G.; Nguyen, P. T.; Ramesh, D.; Booker, L.; Burston, J. J.; Thomas, E. A.; Selley, D. E.; Sim-Selley, L. J.; Lui, Q.; Lichtman, A. H.; Cravatt, B. F. Chronic monoacylglycerol lipase blockade causes functional antagonism of the endocannabinoid system. *Nat. Neurosci.* **2010**, *13*, 1113–1121.
- (10) Cisneros, J. A.; Vandevorde, S.; Ortega-Guti errez, S.; Paris, C.; Fowler, C. J.; L opez-Rodr iguez, M. L. Structure-activity relationship of a series of inhibitors of monoacylglycerol hydrolysis—comparison with effects upon fatty acid amide hydrolase. *J. Med. Chem.* **2007**, *50*, 5012–5023.
- (11) Tarzia, G.; Duranti, A.; Tontini, A.; Piersanti, G.; Mor, M.; Rivara, S.; Plazzi, P. V.; Park, C.; Kathuria, S.; Piomelli, D. Design, synthesis, and structure–activity relationships of alkylcarbamic aryl esters, a new class of fatty acid amide hydrolase inhibitors. *J. Med. Chem.* **2003**, *46*, 2352–2360.
- (12) Labar, G.; Bauvois, C.; Borel, F.; Ferrer, J. L.; Wouters, J.; Lambert, D. M. Crystal structure of the human monoacylglycerol lipase, a key actor in endocannabinoid signaling. *ChemBioChem* **2010**, *11*, 218–227.

(13) Bertrand, T.; Augé, F.; Houtmann, J.; Rak, A.; Vallée, F.; Mikol, V.; Berne, P. F.; Michot, N.; Cheuret, D.; Hoornaert, C.; Mathieu, M. Structural basis for human monoglyceride lipase inhibition. *J. Mol. Biol.* **2010**, *396*, 663–673.

(14) *Glide*, version 5.0.111; Schrödinger, LLC: 2008.

(15) Friesner, R. A.; Banks, J. L.; Murphy, R. B.; Halgren, T. A.; Klicic, J. J.; Mainz, D. T.; Repasky, M. P.; Knoll, E. H.; Shaw, D. E.; Shelley, M.; Perry, J. K.; Francis, P.; Shenkin, P. S. Glide: a new approach for rapid, accurate docking and scoring. 1. Method and assessment of docking accuracy. *J. Med. Chem.* **2004**, *47*, 1739–1749.

(16) *Prime*, version 1.2.3; Schrödinger, LLC: New York, 2007.

(17) Björklund, E.; Norén, E.; Nilsson, J.; Fowler, C. J. Inhibition of monoacylglycerol lipase by troglitazone, *N*-arachidonoyl dopamine and the irreversible inhibitor JZL184: comparison of two different assays. *Br. J. Pharmacol.* **2010**, *161*, 1512–1526.

(18) Muccioli, G.; Labar, G.; Lambert, D. CAY10499, a novel monoglyceride lipase inhibitor evidenced by an expeditious MGL assay. *ChemBioChem* **2008**, *9*, 2704–2710.

(19) Boldrup, L.; Wilson, S. J.; Barbier, A. J.; Fowler, C. J. A simple stopped assay for fatty acid amide hydrolase avoiding the use of a chloroform extraction phase. *J. Biochem. Biophys. Methods* **2004**, *60*, 171–177.

(20) Wang, Y.; Chanda, P.; Jones, P. G.; Kennedy, J. D. A fluorescence-based assay for monoacylglycerol lipase compatible with inhibitor screening. *Assay Drug Dev. Technol.* **2008**, *6*, 387–393.